Materials & Design 209 (2021) 109943

Contents lists available at ScienceDirect

Materials & Design

journal homepage: www.elsevier.com/locate/matdes

Accurate and Computational: A review of color reproduction in Full-color 3D printing

Jiangping Yuan [a,b], Guangxue Chen [a,*], Hua Li [a], Hartmut Prautzsch [b], Kaida Xiao [c]

[a] State Key Laboratory of Pulp and Paper Engineering, South China University of Technology, Guangzhou, China
[b] Institute for Visualization and Data Analysis, Karlsruhe Institute of Technology, Germany
[c] School of Design, University of Leeds, Leeds, UK

HIGHLIGHTS

- Shows the state of the art of color reproduction methods in full-color 3D printing.
- Judges the suitability of current methods expanded to a universal color standard.
- Cases analysis of three key issues for achieving accurate full-color 3D printing.
- States a potential theoretical framework suitable for various 3D printing materials.

GRAPHICAL ABSTRACT

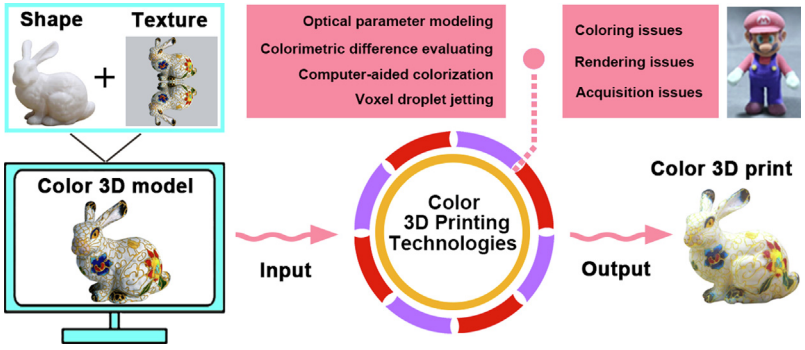

ARTICLE INFO

Article history:
Received 1 March 2021
Revised 12 May 2021
Accepted 27 June 2021
Available online 5 July 2021

Keywords:
3D printing
Color reproduction
Material modeling
Quality evaluation
Digital Fabrication

ABSTRACT

As functional 3D printing becomes more popular with industrial manufacturing applications, it is time to start discussing high-fidelity appearance reproduction of 3D objects, particularly in faithful colors. To date, there is only limited research on accurate color reproduction and on universal color reproduction method for different color 3D printing materials. To systematically understand colorization principles and color transmission in color 3D printing, an exhaustive literature review is stated to show the state of the art of color reproduction methods for full-color 3D printing, such as optical parameter modeling, colorimetric difference evaluation, computer aided colorization and voxel droplet jetting. Meanwhile, the challenges in developing an accurate color reproduction framework suitable for different printing materials are fully analyzed in this literature review. In full-color 3D printing, coloring, rendering and acquisition constitute the core issues for accurate color reproduction, and their specific concepts are explained in concrete examples. Finally, the future perspectives of a universal color reproduction framework for accurate full-color 3D printing are discussed, which can overcome the limitations of printing materials, combined with computational boundary contoning.

Contents

* Corresponding author.
E-mail address: chengx@scut.edu.cn (G. Chen).

https://doi.org/10.1016/j.matdes.2021.109943
0264-1275/

1. Introduction

3D printing is regarded as a revolutionary technology for customized fabrications. With the increasing functionality of printed parts, 3D printing techniques have been widely applied in, e.g., aerospace engineering, automotive electronics, biomedicine, cultural creativity, and geographic information industries to manufacture complex components and special parts with competitive performance [1–5]. Besides material formulation, microstructure optimization and mechanical properties, which are in the foreground in these applications, the surface colors of 3D printed objects are important and do no longer meet modern aesthetic and practical needs [6,7]. Since 2014, color 3D printing techniques emerged mainly for multicolor 3D visualizations with powder-based 3D printers produced by 3D-systems [8], paper-based 3D printers produced by MCOR-technology [9], and plastic-based 3D printers produced by Stratasys [10]. According to the ISO/ ASTM 52900, there are seven general principles for additive manufacturing processes, as shown in Fig. 1 [11]. Those color 3D printing techniques mentioned above realize the binder jetting (BJ), sheet lamination (SL), and material jetting (MJ) principles, respectively. While vat photopolymerization (VPPM) based color 3D printers are also capable of reproducing a wide range of colors, their color reproduction performance is not as good as material jetting based printing [12]. Color reproduction on the VPPM type is achieved by curing the entire surface of each light-curing resin layer using multiple linear curing arrays, which limits color mixing and pigment path distribution [13,14]. Color 3D printing devices based on the three remaining principles in Fig. 1, e.g., material extrusion (ME), powder bed fusion (PBF), and direct energy deposition (DED) have been developed first with material chambers and then with printing or extrusion heads, but their color reproduction capabilities are also far from satisfactory [15–17]. There are benchmarks for 3D printing quality evaluation [18–20], but benchmarks such as standardized test sets, measurement and viewing conditions for evaluating color 3D printing setups are ignored. Combined with the

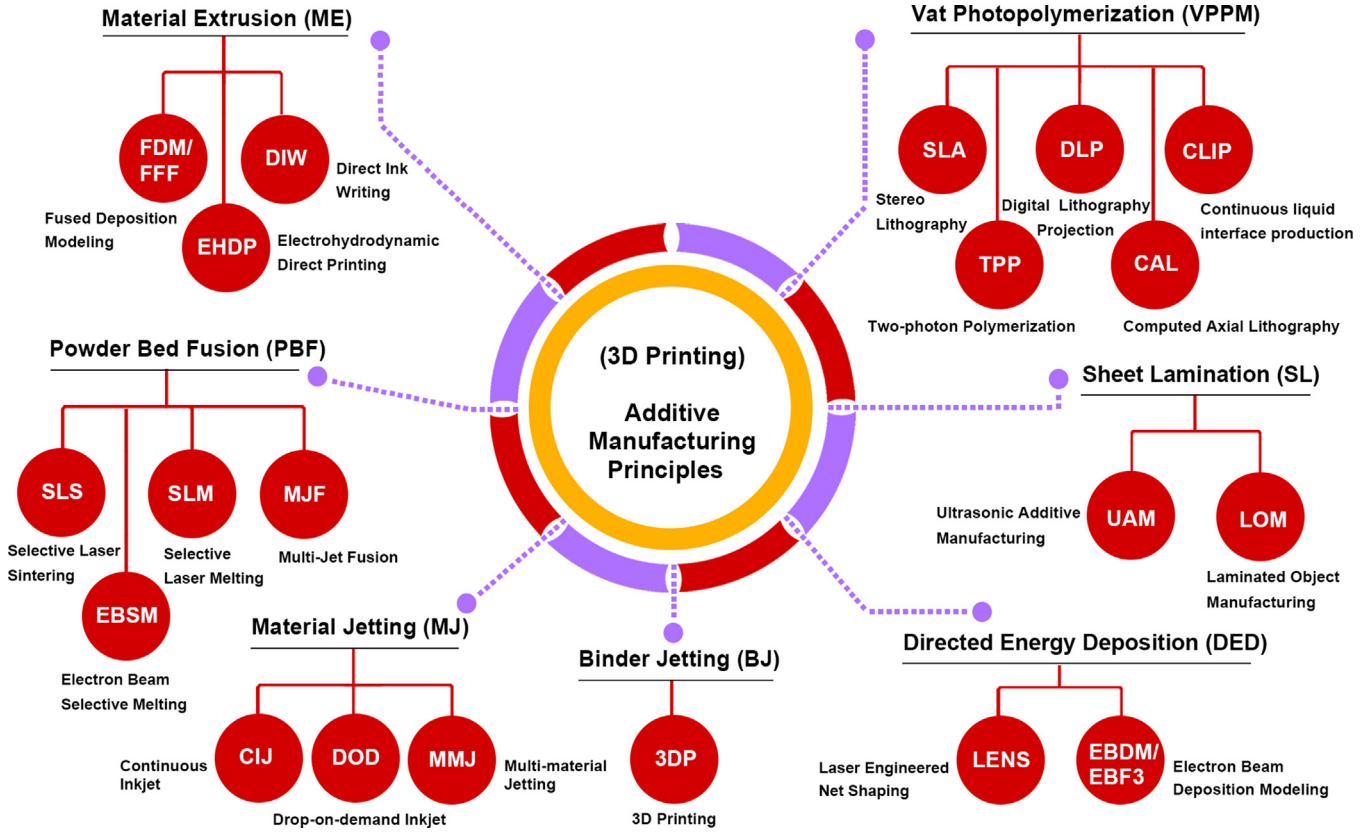

Fig. 1. Comparison of kernel processes used in color 3D printers.

above literature analysis, the fundamental reason for the slow progress in accurate color reproduction of current 3D printing devices can be summarized as a lack of a universally accepted color reproduction theory and an evaluation system [21].

Moreover, the diversity of principles, technologies and materials used in existing color 3D printing techniques has led to the situation where further developments happen scattered across different fields. Mainly, there are 3D printing device developers in manufacturing and computer science, 3D printing materials scientists, and color scientists in the fields of printing and optics working on what is commonly called color or multicolor 3D printing [22–24]. In order to stress that an accurate and realistic appearance reproduction of 3D objects is more than just multicolor printing, a terminology full-color 3D printing is suggested for this advanced area of 3D printing that provides more accurate reproduction [25]. In full-color 3D printing, the color of each point on a printed object should be accurately reproduced, but current processes don't really achieve this goal. This is geared towards personalized fabrication that requires fine color gradations in the target area. However, the full-color 3D printing also suffers from printing speed and build size for mass production [26].

Moreover, consistent with different printing substrates, there are paper-, plastic-, powder-, metal-, food- and organism-based full-color 3D printing processes [27]. The color of full-color 3D printed objects is perceived from the absorption and reflection characteristics of the selected coloring substrates. For non-scattering materials (e.g., transparent inks), this follows the principle of subtractive color mixing [28,29].

Color appearance of subtractive color mixing of 2D printer can be accurately predicted by colorimetric measurement standardized by the International Commission on Illumination (CIE) with LUT-based color characterization model recommended by the International Color Consortium (ICC) [30]. However, it is not actually effective for full-color 3D printing, although both 3D printing and 2D printing utilize digital discretization for color transmission [31]. The key discrepancies are illustrated in detail in Fig. 2. The arrows on the left side in the upper and lower row, respectively, symbolize the digital discretization process in 2D printing. Meanwhile, the digital discretization process for 3D printing can be divided into two steps: the first step is similar with that in 2D printing; the second step is illustrated by the arrow on the right side in the upper row. It should be noted that these two steps are directly integrated into the slicing process of color 3D printing systems.

Obviously, the lack of a unified and accepted accurate measurement theory allowing to evaluate color reproduction quality for full-color 3D printed products is a challenging problem [32]. The principles followed by color measurement tools in 2D printing are not applicable to color 3D entities. In Fig. 3, the essential differences are demonstrated: The Fig. 3 **(a)-(c)** demonstrate the light path transmission for conventional print, irregular print, and color 3D print with a standard measurement combination of a 0° illumination angle and a 45° viewing angle (Short for 0°as45°). In Fig. 3 **(b)**, a measuring instrument would not correctly measure the angular and spectral distribution of the reflected light at the measurement point with this viewing angle. Moreover, in Fig. 3 **(c)**, the angular and spectral distribution of the reflected light changes even more dramatically than that in Fig. 3 **(b)**. Practically, a spectrophotometer with an integrated sphere can improve measurement accuracy, but the problems above cannot be overcome when the geometry of the 3D printed sample is more complex with a large number of tiny colored curved surface with spatial irregularities and uneven optical features. Meanwhile, the X-Rite research center performed a measurement survey for color pigments stacked on flat prints and reported changes under different viewing and illumination angles as shown in Fig. 3 **(d)-(f)** [33]. Fig. 3 **(d)** & **(e)** vividly illustrate all standard combinations available for current measurement instruments while Fig. 3 **(f)** shows the results obtained by four different color measurement instruments with these angle combinations for the same sample point. To meet the demand for better measurements, instruments with a wider range of standard angle combinations are constantly being developed in color science.

In addition, a precise measurement mechanism to develop full-color 3D printing with accurate color reproduction is still unknown. So far, color evaluation is mostly based on chromaticity differences in flat areas. However, under the current limitations on illumination and viewing angles, measurement deficiencies are still prevalent. Material appearance reproduction is discussed in the proceedings of the 27th Color and Imaging Conference published by the Society for Imaging Science and Technology in 2015 [34]. These discussions show that material appearance can be regarded as a visual sensation reproduction, which indicates that the accuracy of color reproduction is affected by other aspects, such as size, texture, gloss, transparency, and opacity. A typical example for current efforts is the European Union's Horizon 2020 research and innovation program led by the Norwegian Color and Visual Computing Laboratory with the goal to explore reproducing and measuring material appearance [35]. Achieving and controlling accurate color reproduction of full-color 3D printing is a tricky interdisciplinary issue although some practical models and specific theories have been developed in industrial manufacturing, artistic aesthetics, color science and computer science [36,37].

In this review, the discrepancies in current color reproduction as well as in color measurement on the one hand and evaluation on the other are both elaborated. In Section 2, the state of the art of color reproduction methods in full-color 3D printing based on

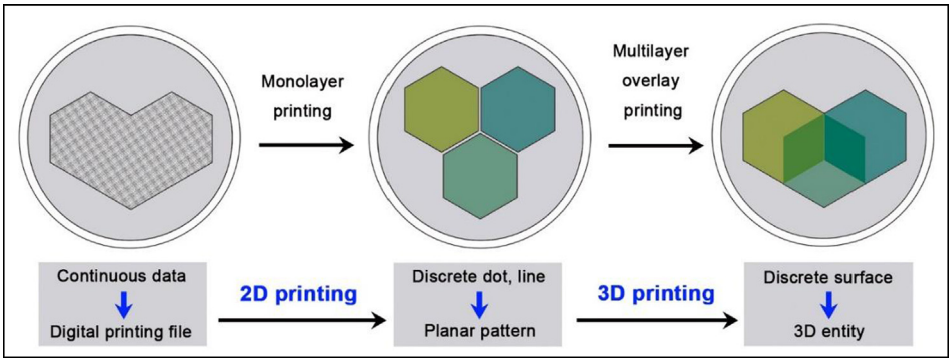

Fig. 2. Digital discretization in 2D printing and 3D printing.

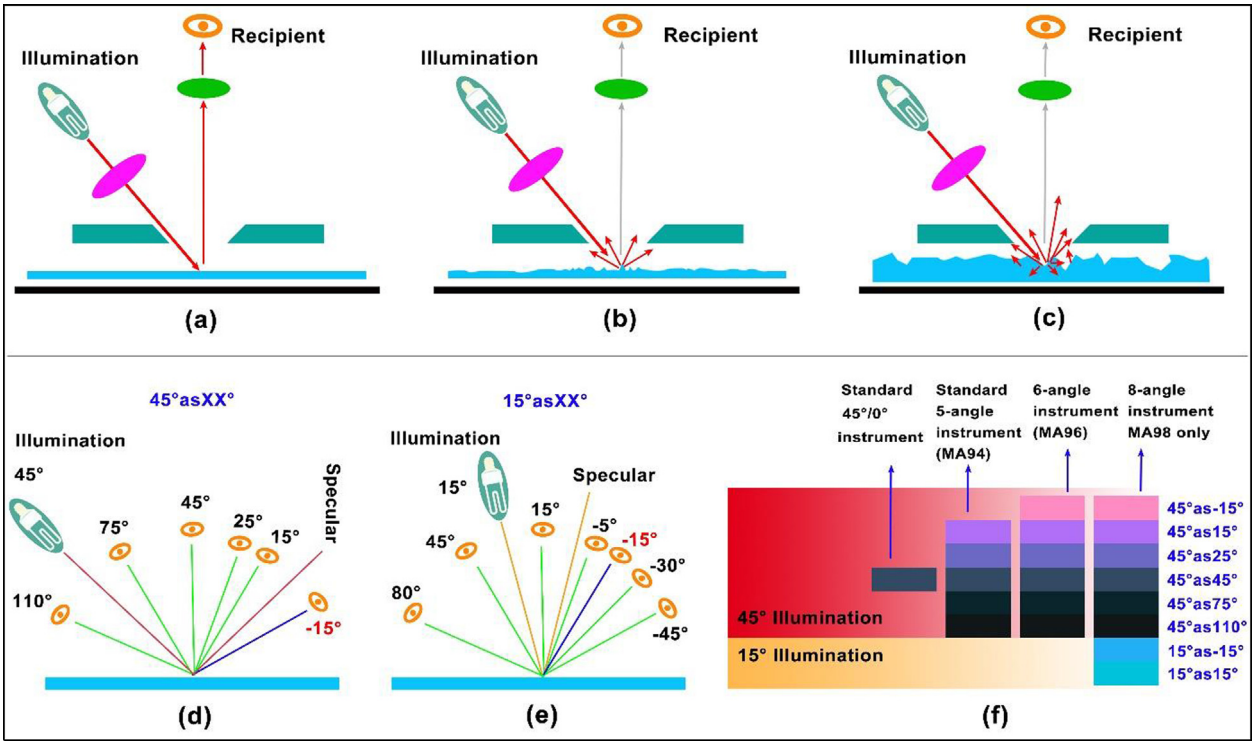

Fig. 3. Schematic diagram of measurement variances and influencing factors for opaque objects: **(a)** smooth or flat substrate measurement with single illumination and viewing angle; **(b)** uneven or irregular substrate measurement with single illumination and viewing angle; **(c)** color 3D object measurement with single illumination and viewing angle; **(d)** color patch measurement with 45° illumination and multi-viewing angles; **(e)** color patch measurement with 15° illumination and multi-viewing angles; **(f)** color comparison of different measurement angles under two types of illumination.

specific printing substrates is presented in detail. In Section 3, core accuracy issues in color transmission for full-color 3D printing and 2D printing are compared with theoretical examples. Finally, the enlightening perspectives are also given for exploring the research highlights with the potential for a universal accurate color reproduction in cross-substrate full-color 3D printing.

2. Overview of color reproduction methods

In this section, an overview of existing color reproduction methods used in full-color 3D printing is presented. In terms of color transmission, these methods can fall into the following four subcategories "optical parameter modeling", "colorimetric difference evaluation", "computer-aided colorization", and "voxel droplet jetting". In principle, optical parameter modeling and colorimetric difference evaluation are synthetic tools based on theoretical results in optics while computer-aided colorization and voxel droplet jetting are developed by analyzing printing results and behavior.

2.1. Optical parameter modeling

Optical parameter modeling used physical measurements and is based on multivariate functions describing radiative light transfer performances from arbitrary 3D objects illuminated by a given light source. In general, these radiative transfer performances mainly consist of light reflection, light refraction, light diffusion, and light diffraction [38]. In terms of transmission properties of printing materials, any 3D object can be divided into transparent, translucent, and opaque geometries [39]. Light reflection of opaque 3D objects and light transmission of transparent 3D objects can be easily measured by current standard optical devices whereas light transmission of transparent materials is characterized by total light refraction accumulation. For a translucent 3D object, light diffusion is used when there are many changes and few separations anisotropic media, while light scattering is used a small number of changes in the medium and more distinct separations [38,39]. However, the light diffraction predictions are rarely studied for printing materials.

Importantly, it is the accurate modeling of light scattering from translucent objects that is the central challenge of color rendering of materials yet to be solved in computer graphics, especially for anisotropic and heterogeneous translucent materials [40]. Light scattering from translucent materials can be divided into planar scattering and volumetric scattering in terms of the number of shape dimensions [41]. Since the fabricated objects usually belong to 2.5- and 3-dimensional material rendering, volumetric rendering prediction and its optical density material approximation distribution have become a research hotspot in the field of computer graphics [42]. The works by Théo Phan Van Song on four-flux volume scattering models allows for color prediction of 2.5D printed objects for different thicknesses and color inks using colorimetric and spectral data [43–46]. In addition, with the development of texture mapping functions for translucent materials, high-resolution appearance description models for translucent 3D objects with isotropic scattering parameters is simulated by bidirectional scattering distribution functions (BSDF) [47,48]. To combat the edge-loss in reflectance measurement on translucent materials including colored and opalescent materials, an improved bidirectional scattering-surface distribution functions (BSSDFs) is proposed for comprehensive numerical simulation of translucent appearance in [49]. The BSSDFs, which consist of bidirectional scattering-surface reflectance distribution functions (BSSRDF) and bidirectional scattering-surface transmittance distribution functions (BSSTDF), are difficult to measure, to store, and to compute [50]. Since the effective scattering distance of most commercial

printing materials for 3D printing is substantial, the strategies used with the models above mainly rely on local pure scattering control with the result that visible inaccuracies become more apparent on color 3D printed parts [51]. Subsequently, scattering-aware texture reproduction for planar 3D prints had been developed by an iterative optimization scheme controlling a fully volumetric material distribution and a commercial five-tone 3D printing process. Two years later, this method has been extended to arbitrarily shaped objects by a full-fledged optimization on a small domain to effectively compensate for internal light scattering [52]. These models are well studied in 3D object rendering, but are poorly investigated in high-fidelity full-color 3D printing.

Undoubtedly, color reproduction models adopting light reflections for opaque 3D objects have always been mainstream techniques in full-color 3D printing. Classical models include the Blinn-Phong model, Ward or Cook-Torrance model, and simple bidirectional reflectance distribution function (BRDF) models [53–55]. With the development of texture mapping functions for opaque 3D objects, high-resolution appearance description models for even more complicated 3D geometries were formed by the spatially varying BRDF (SVBRDF) [56,57]. Moreover, microfacet modeling is widely applied to realistic surface appearance measurement applications [58].

Typically, the State Key Laboratory of Modern Optical Instruments at Zhejiang University in 2013 reviewed recent BRDF models applied to appearance measurements of colored 3D freeform models and proposed a realistic color rendering method for 3D objects with a quantifiable appearance reproduction [59]. In the French National Metrological Institute for radiometric and photometric quantities (LABORATOIRE NATIONAL DE METRILOGIE ET ÉSSAIS (LNE), an independent research institute), a program measuring the BRDF specular peak was started in 2008 to explore the precise measurement of gloss attributes, and launched a lab facility named Conoscopic Device for Optic Reflectometry (ConDOR) around 2015 [60]. As its core member, Gaël Obein formed a new optical measurement team at the Conservatoire National des Arts et Métiers (CANM) to further develop a new and large 3D scanning device (3D-DEMO) to capture the material appearance of arbitrary 3D objects with complex surface properties. The 3D-DEMO enables to measure a wider range of illumination and viewing angle combinations with a 5° resolution, than the CIE recommend for 2D printing [33]. It greatly enriches and improves acquisition accuracy for surface appearance of complex color 3D objects including color, texture, and gloss. Worldwide, this huge and costly device is unparalleled in its quality measurements by other machines. However, the measurement process is time-consuming and requires a large memory space. For example, the appearance acquisition time of a common basketball surface takes about 8 h, and its raw data reaches 1.5 TB when stored in the full bidirectional texture function (BTF) format (e.g., chunked data).

Subsequently, the X-Rite, a leading United States-based color measurement equipment company developed a portable commercial hemispherical 3D object appearance acquisition prototype providing multiple illumination angles and viewing angles in 2016, naming TAC7 3D scanner. Apart from utilizing color measurement principles of 2D printing, the output data of this 3D scanner can either be saved as a sparse BTF or a SVBRDF normal map. To better understand the critical advances in optical parameter modeling, the corresponding data acquisition and transformation is illustrated in Fig. 4. Compared to the BRDF, the SVBRDF has an additional bivariate mathematical function, which enables the representation of planar textures on opaque materials. The BRDF is sufficient for acquiring functional material appearances for plastic- and metal-based 3D prints, while the appearance reproduction of multi-material 3D printed products with color complexity must use the SVBRDF. Fig. 4 **(d)** stands for combining dense illumination and viewing angles in a color 3D scanning instrument. Of course, combining illumination and viewing angles in an instrument, their numbers need to be balanced, meanwhile, larger numbers mean more accuracy but less efficiency. In Fig. 4 **(g)** & **(h)**, the color perception of a sample appearance is significantly different from each other, for instance, the material appearance of the color 3D object captured by the 3D-DEMO is more saturated and brighter. Conversion between full BTF, sparse BTF and conventional digital format is possible, but each conversion has a loss of color information.

For the TAC7 3D scanner, the X-Rite color research group developed a new appearance exchange format (AxF) based on the planar color exchange format (CxF) used in the ISO117972 standard, which consists of a diffuse albedo map, a specular roughness

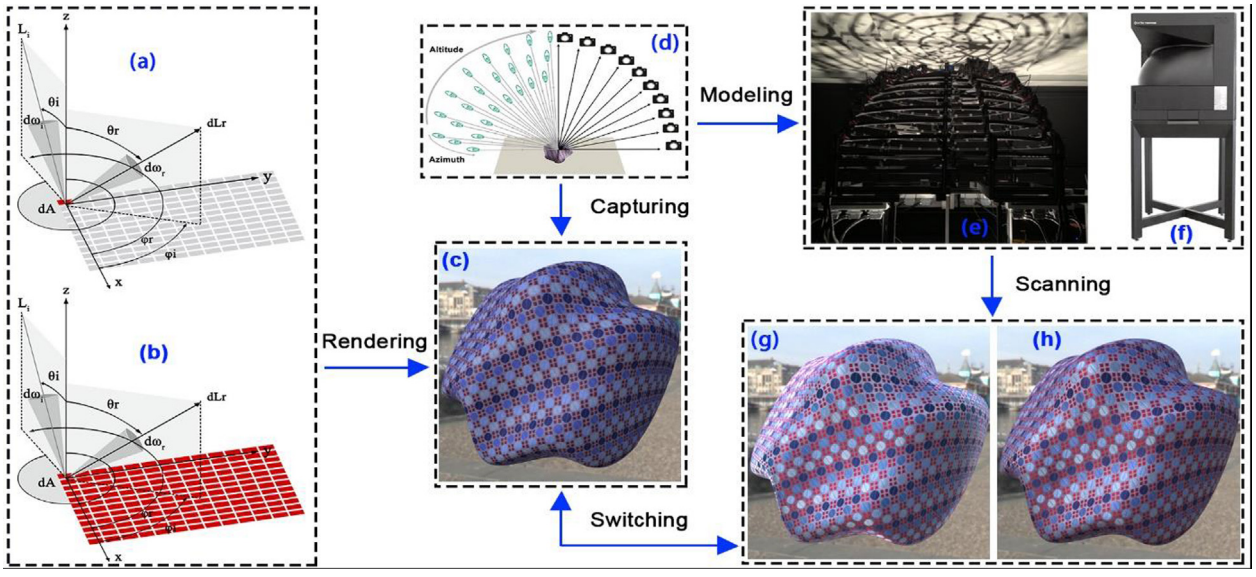

Fig. 4. The data acquisition and transformation in optical parameter modeling: **(a)** BRDF model; **(b)** SVBRDF model; **(c)** conventional digital format; **(d)** acquisition with multi-viewing and illuminating angles; **(e)** 3D-DEMO scanner; **(f)** TAC7 scanner; **(g)** full BTF captured by 3D-DEMO scanner; **(h)** sparse BTF captured by TAC7 scanner. Modified examples used with permission from [33], copyright (2016) X-Rite.

map, a specular color map, a normal map (replace bitmaps as needed), a surface orientation map (to capture anisotropy), a height map (also known as displacement map), a Fresnel map, an index of refraction map, an alpha map and car paint (CPA) [33]. The first version of the TAC7 3D scanner and its AxF format was formally released at the ICC 3D Display and Color 3D Printing symposium held at Taipei City in 2016, but was not recommended by most of ICC technical committees due to its high price and suboptimal accuracy for measuring colored 3D objects with complex gloss and transparency. Meanwhile, like the AxF structure, a surface appearance description tag is defined and embedded into the iccMAX profile to construct the chromatic Ward BRDF model consisting of multiple illumination angles and viewing angles [61]. Later, an internal ICC technical committee for appearance acquisition and measurement of colored 3D objects was established with the X-Rite research center.

Further, the 3D manufacturing format (3MF) is a 3D print file format with color attributes has been developed by a key industry consortium led by Microsoft. It is widely used in additive manufacturing and physical visualizations of digital material. The mainstream manufacturers of color 3D printers have been promoting this format since 2015 [62]. For instance, the HP 3D printing division implemented this format to all its color 3D printer series in 2016. Likewise, MCOR-technology Inc. used it for their relative color 3D printing software in 2018.

Optical parameter modeling provides more accurate optical measurements and color appearance description formats for 3D printing, which affects the surface color output. Based on the texture image gamut mapping principle, algorithms and frameworks for color gamut mapping and gloss mapping are used to explore accurate surface reproduction of 3D printed objects [63,64]. This technique helps to improve the color reproduction accuracy of full-color 3D printing given pure translucent materials but fails when it comes to reproduce colored 3D objects with high gloss materials. Because the combined effects of shape and material properties is poorly understood, the optical parameter modeling is still difficult to set up an accurate color reproduction method for all types of 3D printing materials.

2.2. Colorimetric difference evaluation

Colorimetric measurements are used to evaluate full-color 3D printing. They are based mainly on numerical minimization of color differences to match the visual perception of the human eye. So far, they are not used to automatically adjust the printing parameters or to pretreat the input for current full-color 3D printers, yet the advantages of a colorimetric measurement are its simplicity, speed and low-cost, but it does not work well with transparent or glossy multi-jetting materials [65,66].

Significantly, the color quality of 3D printed objects has been improved continuously by minimizing color differences in full-color powder-, plastic- and paper-based 3D printing. In 2012, Maja Stanic at the University of Zagreb in Croatia printed a highly saturated artwork with the Z510 powder-based 3D printer and measured CIE L*a*b* values on selected smooth surface segments of the printed model with the Gretag-Macbeth XTH spherical spectrophotometer [67,68]. The printed surfaces presented vivid colors in the reproduced artwork. Maja Stanic developed a metric using the CIEDE2000 color difference formula and further proposed a color compensation lookup table for powder-based 3D printing tests to provide direct color selection for general 3D printing users.

In 2013, Kaida Xiao et al. from the University of Liverpool printed soft prostheses by the SLA 3D printer and took the Minolta CM-2600D spectrophotometer to measure the CIE ΔE^*_{ab} values of surface color points on the facial prosthesis shown in Fig. 5 **(a)**. Further, they optimized the color reproduction consistency for biolog-

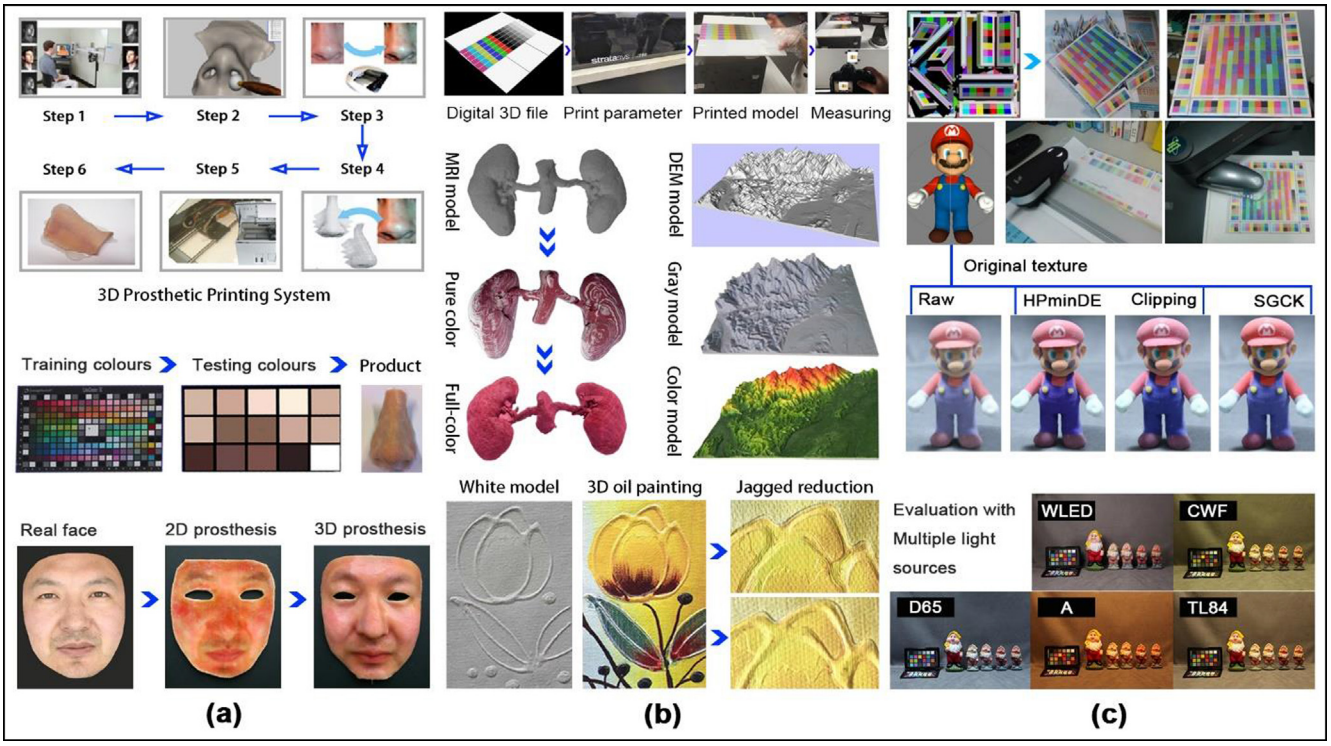

Fig. 5. Examples for color reproduction optimization based on colorimetric differences:**(a)** Kaida Xiao group; **(b)** Guangxue Chen group; **(c)** Pei-li Sun group. Examples used with permission from [71], copyright (2014) Springer Nature; [72], copyright (2014) the authors; [77], copyright (2018) Society for Imaging Science and Technology; [78], copyright (2016) the author; [80], copyright (2018) the author; [81], copyright (2015) SPIE; [82], copyright (2016) Society for Imaging Science and Technology; [83], copyright (2016) the authors.

ical tissues by a multi-parameter feedback framework [69–72]. In the upper part of Fig. 5 **(a)**, their 3D prosthetic printing system is illustrated. It consists of the following six steps: 3D image acquisition, 3D image design, color management, color texture mapping, 3D color printing, post processing. The lower part of Fig. 5 **(a)** shows the color test chart used in their multi-parameter feedback framework and the effect of the imported objects on facial replication.

Since 2013, the color 3D printing group led by Prof. Guangxue Chen at South China University of Technology focused on the color reproduction theory and the process optimization for paper-based full-color 3D printing with the MCOR IRIS 3D printer and the MIMAKI UV-photocurable 3D printer for applications in the cultural creativity industry [73–77]. Based on a colorimetric difference evaluation, this group explored accurate color reproduction strategies of A3 paper-based 3D printing (The latest MCOR paper-based 3D printer uses A4 paper) for precise visualization of surgical models (originate from MRI data), military 3D maps (originate from DEM data) and improved high-fidelity reproduction of expensive 2.5D oil paintings (originate from 3D scanning data) [78–80], see Fig. 5 **(b)**. Compared with current sequential printing of color sliced layers using four primary color inks, this group proposed a new computational framework to adjust the order and amount of sliced color layers and transparent layers to attenuate the jagged boundary effect of UV-photocurable 3D printed objects, as shown in the lower part of Fig. 5 **(b)**. This framework implemented staircase effect mitigation with a fixed sliced layer thickness by a material jetting 3D printing process with a printing accuracy of 10 μm providing new ideas for optimizing surface reproduction in other 3D printing processes on a bigger printing scale.

In the period 2015–2016, Pei-Li Sun et al. at the Institute of Color and Vision of the Taiwan University of Science and Technology attempted to minimize color differences to improve the accuracy of color reproduction for plastic-based color 3D printing [81–83]. The Fig. 5 **(c)** depicts 3 different specific studies with a BJ-type full-color 3D printer: (1) A puzzle-like omni-directional color test target for estimating color variations across different surface directions. The measuring results can be used to reduce the color variations (See the upper part of Fig. 5 **(c)**). (2) Gamut mapping from sRGB display to 3D prints shown in the middle part of Fig. 5 **(c)**. The result shows SGCK (chroma-dependent sigmoidal lightness mapping and cusp knee scaling) model is preferred to Clipping (minimum ΔE clipping) and HPminDE (hue preserved minimum ΔE clipping). (3) Minimize color differences across 5 important illuminants shown in the lower part of Fig. 5 **(c)**. The result is evaluated by the perceptual differences and shows D65 illuminant shows better preference. These test targets can provide an efficient reference for regular colored 3D prints, but don't take into account color variations in the build orientation. In addition, SGCK is not necessarily the best algorithm for color reproduction among the color gamut mapping algorithms for texture images.

In 2016, Gui-Hua Cui et al. at Wenzhou University proposed a color difference prediction framework by calculating surface chromatic values of 3D printed objects with psychological scale experiments to evaluate and optimize the color finally reproduced. This prediction framework originated from inherently imperfect color difference models (CIE ΔE^*_{ab}, CIE ΔE^*_{00}) in 2D printing, whose number of flat color blocks printed by paper-based full-color 3D printing is too small [84]. Currently, no numerical computational model has been constructed for this prediction framework.

In order to accelerate the progress in global standardization of accurate color reproduction, the CIE 8th Division appointed the 8–17 technical committee (CIE TC 8–17: Methods for Evaluating Color Difference between 3D Color Objects) to develop formal color difference evaluation methods for color 3D objects in 2017 for a six years period [85].

Besides, colorimetric difference evaluation methods have also been developed for other substrates. For example, a color research group at Wuhan University presented a complete dye matching reproduction framework for digital printing on textiles using the Kubelka–Munk theory, which can be extended to the 3D printing of textiles [86]. Further, the 2.5D appearance reproduction evaluation method and the relative ink droplet characterization of elevated printing was analyzed by the Océ-Canon company in the Netherlands [87,88]. The core idea behind colorimetric difference evaluation is to match points on the smooth regions of printed objects to minimize their color differences. However, sampling color points only on smooth areas does not always cover key or complex color features, because colorants are more difficult to print precisely on rough than on smooth regions. Optical properties such as gloss, transparency and texture are challenging in integrating a color difference evaluation model for different coloring materials [89]. Although the principle of colorimetric difference evaluation is well-known in 2D printing to optimize color reproduction, applying this principle to the full-color 3D printing to achieve accurate color measurements for complex 3D curved surfaces with existing color measuring instruments remains a big challenge.

2.3. Computer-aided colorization

Computer-aided colorization is an indirect technique for accurate color reproduction of 3D printed objects based on the combination of computer geometry simulation and digital colorization. It can be categorized into computational transferred printing, computational block coloring and computational contour inkjet printing. In the following, these sub-categories are explored in more detail. There are two computational transferred printing techniques: the computational hydrographic printing (CHP) and computational thermoforming printing (CTP).

Generally, hydrographic printing refers to a unique color reproduction method controlled by computational texture registration algorithms that transfer accurately printed high-resolution color patterns on a thin film to the designated surface of the 3D objects to be manufactured. The principle of traditional hydrographic printing is that printed polyvinyl alcohol (PVA) film tiles on a water tank with room temperature wrap around the desired object until it is fully covered. Subsequently, the object together with the film is rotated several times in the water in only one direction [90]. The traditional hydrographic printing is a simple and economical method that enables the color features of complex geometries produced with a wide range of materials in high quality. Nevertheless, it is still difficult to accurately apply color textures to printed 3D objects with doubly curved surfaces.

Noteworthy, the low-cost and efficient computational framework shown in Fig. 6 **(a)** to calculate the precise stretch and distortion of the printed color pattern on transfer films has been proposed primarily by the State Key Lab of CAD&CG at Zhejiang University [91]. Accurate surface color texture alignment is computed by simulating the transfer film and executing it by a precise calibration system controlled by a semiautomatic mechanical apparatus with a 3D vision capturing device. In computational hydrographic printing, they achieve vivid color reproduction in three steps: (1) First, one prints an achromatic 3D model; (2) second, a suitably distorted texture is printed on a PVA film by 2D inkjet printing; (3) third, the film is oriented, dipped into water with room temperature and finally transferred to the printed object. On the tiger mask in the lower part of Fig. 6 **(a)**, two red marked areas are compared to show how the film thickness

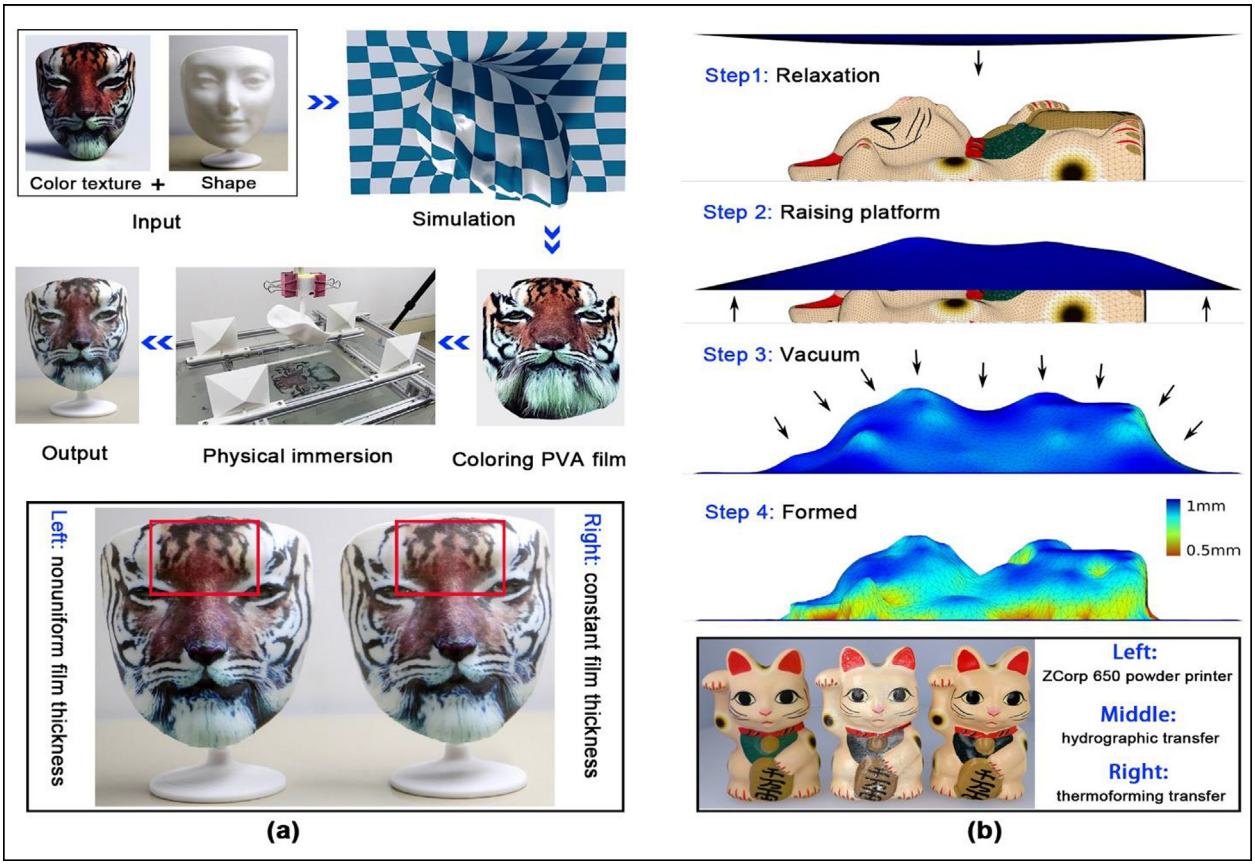

Fig. 6. Computational transferred printing workflow and it output comparison: **(a)** hydrographic printing; **(b)** thermoforming printing. Examples used with permission from [91], copyright (2015) Association for Computing Machinery (ACM); [92], copyright (2016) ACM.

influences the color reproduction of 3D objects by two simulated hydrographic films.

On the other hand, computational thermoforming utilizes the melting decomposition of a printed plastic sheet to transfer the attached ink to the designated surface. The computational thermoforming method was developed and improved jointly by a research group at the ETH Zurich and a group at the Disney Research Centre [92]. This method provides a simulation algorithm to convert a textured digital 3D model into a 2D image printed on the plastic sheet prior to pyrolysis. The upper part of Fig. 6 **(b)** illustrates the three phases of thermoforming simulation and the finally formed result. The color of the dark blue sheet visualizes the thickness of the simulated plastic sheet, changing from 0.5 mm to 1.0 mm. On the bottom of Fig. 6 **(b)**, this method is compared to the powder-based 3D printing technique and hydrographic transfer technique for a Plutus cat. The computational thermoforming replica showed a higher resolution than powder-based 3D print, but fewer artifacts in its flat regions than that reproduced by the hydrographic technique. However, this fabrication technique is prone to color deterioration issues due to high temperature and vacuum suction. In summary, it should be stated that the computational transfer printing is not available for 3D printed entities that are sensitive to water or heat. It must be said that computational hydrographic printing and thermoforming printing are good for color reproduction of oversized 3D objects formed by general 3D printers and ordinary inkjet printers at very low cost.

With respect to computational block coloring, it is a new way to meet accurate color reproduction for large-sized 3D entities with concave and convex surface areas, based on surface segmentation algorithms and splicing strategies. The principle of computational block coloring is also ideal for complex 3D objects with microstructures. Joint research efforts at the University of Cagliari and New York University led to several decomposition techniques: a disjoint decomposition into height-field blocks, volumetric decomposition, surface segmentation, and axis-aligned height-field segmentation [93]. These techniques have been applied to the FDM (Fused Deposition Modeling) 3D printers for large-scale pure-color rather than gradient-color 3D models. The axis-aligned height-field segmentation provides a potential way to achieve cheaper color 3D prints and its key steps are illustrated in Fig. 7 **(a)**. This segmentation scheme may result in a decrease in the final forming efficiency and overall strength due to too many segmented sub-blocks. Previously, Jiangping Yuan et al. from the South China University of Technology proposed a 3D cutting & bonding frame (3D-CBF) method for full-color paper-based 3D printing, which can be integrated into the slicing phase [94,95]. Fig. 7 **(b)** shows cutting angle settings and layout options for a cuboid model with specific color features to test the adaptability of the proposed 3D-CBF for complex cases. In Fig. 7 **(c)**, the effect of three cutting angles and five adhesive brands on each 3D printed banana model is demonstrated in detail. In addition, the effect of five bonding temperatures on the physical visualization of banana with Garefu-brand adhesive and 90°cutting angle was evaluated by its bonding strength and surface smoothness. Based on all the above cases, strategies for subblocks decompositions can help to reduce the difficulty of accurate color reproduction.

Likewise, computational contour inkjet printing is adapted inkjet printing to transfer the color of a filament to the contour of any layers by an additional melting process. The original purpose of this method was to develop practical paths by unitizing

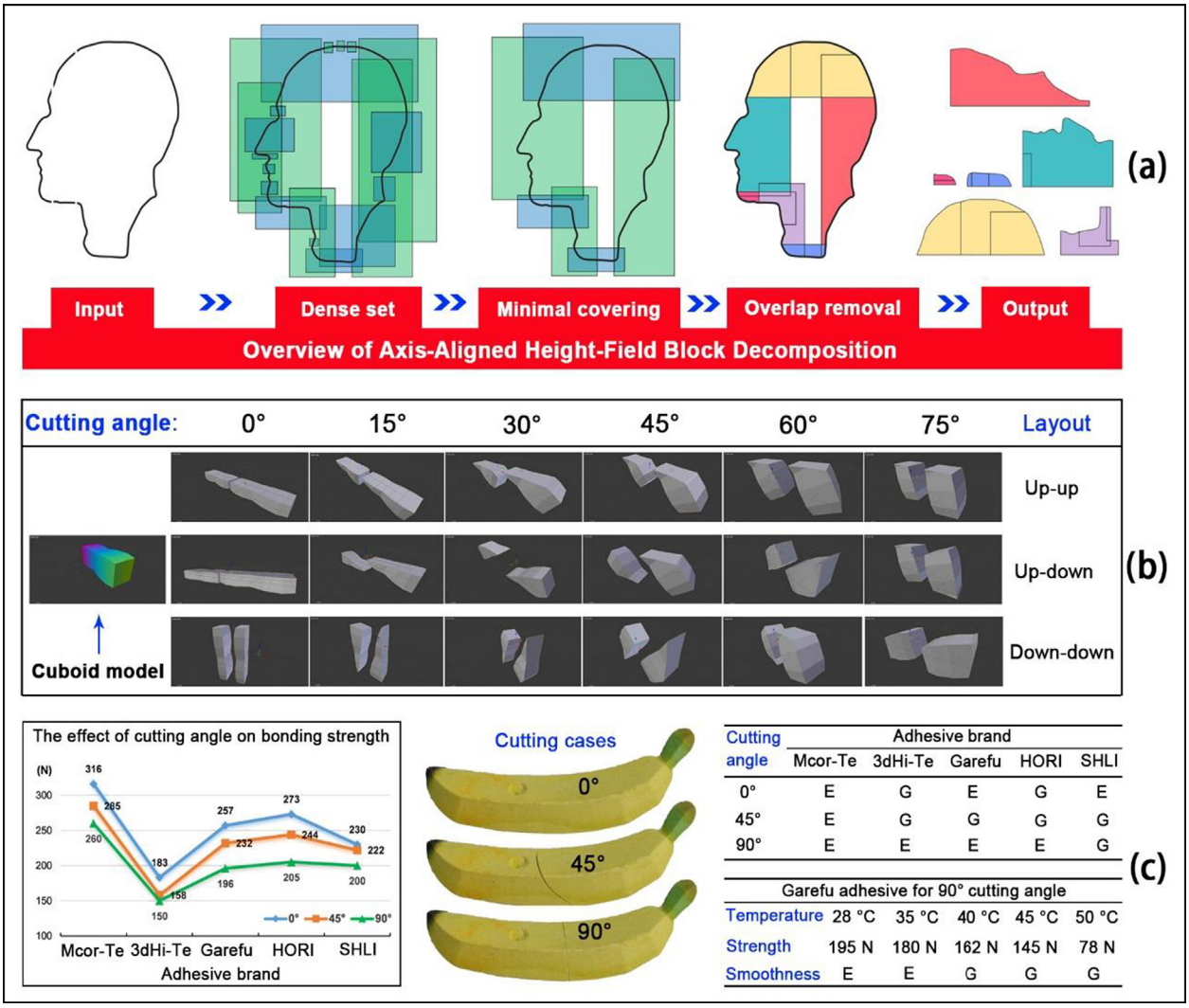

Cutting angle	Adhesive brand				
	Mcor-Te	3dHi-Te	Garefu	HORI	SHLI
0°	E	G	E	G	E
45°	E	G	G	G	G
90°	E	E	E	E	G

Garefu adhesive for 90° cutting angle					
Temperature	28 °C	35 °C	40 °C	45 °C	50 °C
Strength	195 N	180 N	162 N	145 N	78 N
Smoothness	E	E	G	G	G

Fig. 7. Strategies for color 3D object decomposition: **(a)** axis-aligned height-field segmentation; **(b)**~**(c)** 3D cutting & bonding frame method. Examples used with permission from [93], copyright (2018) ACM; [94], copyright (2017) Emerald; [95], copyright (2017) Springer Nature.

customized color filaments and a single spray nozzle to improve color reproduction accuracy of the FDM 3D printer. The prepared color filaments were colored by certain conventional 2D printing processes. The color position on the filament is computed to match the target color position on the contour of each printed color layer. At Jinan University, Yang et al. presented a new method for the multi-color FDM 3D printing process with color adherences produced by silk-screen printing, based on the principle of low-dimensional colorization [96]. Its limitation is that the surface color of the next layer is susceptible to inevitable pollution by residual colorants in the operating nozzle. Moreover, Jennifer Lewis's group from the Harvard John A. Paulson School of Engineering and Applied Sciences proposed a spray regulator for a single nozzle to quickly distribute voxelized droplets of multiple coloring materials. This device has specific microfluidic structures installed in the print nozzle to switch and combine up to eight basic coloring materials while avoiding residues at the nozzle [97]. One device can integrate 128 nozzle-based arrays to print 128 gradient colors at the same time, which provides better color control for the computational contour in using multi-liquid coloring materials.

In general, computer-aided colorization allows better color reproduction in plastic-based full-color 3D printing. For paper-based full-color 3D printing, the computational block strategies seem to promise more accurate color reproduction. How to simulate and compute the colorization flow in each bonding paper sheet is another important issue. Taking binder jetting as an example, to improve the color reproduction accuracy of powder-based full-color 3D printing by contour coloring, one still needs to fully understand how powder particles behave under their formation and how color pigments penetrate them. Then together with advanced algorithms, accurate full-color 3D printing for various printing materials may become possible with this method.

2.4. Voxel droplet jetting

Since 2015, a new data-driven method which can be defined as the voxel droplet jetting, has been developed for higher accuracy in full-color 3D printing by computing discrete ink droplets at voxel-level. This has been applied rapidly in the field of customized colorful geometries due to its precision close to conventional 2D printing with advanced color separation methods and printing heads. For example, commercial 2D printing heads from worldwide companies such as Epson, Fuji, Konica Minolta, Kyocera, Panasonic, Ricoh, Toshiba, Xaar etc., can be also customized for color 3D printers. Fig. 8 shows respective examples and specific principles for the voxel unit generation of full-color 3D printing.

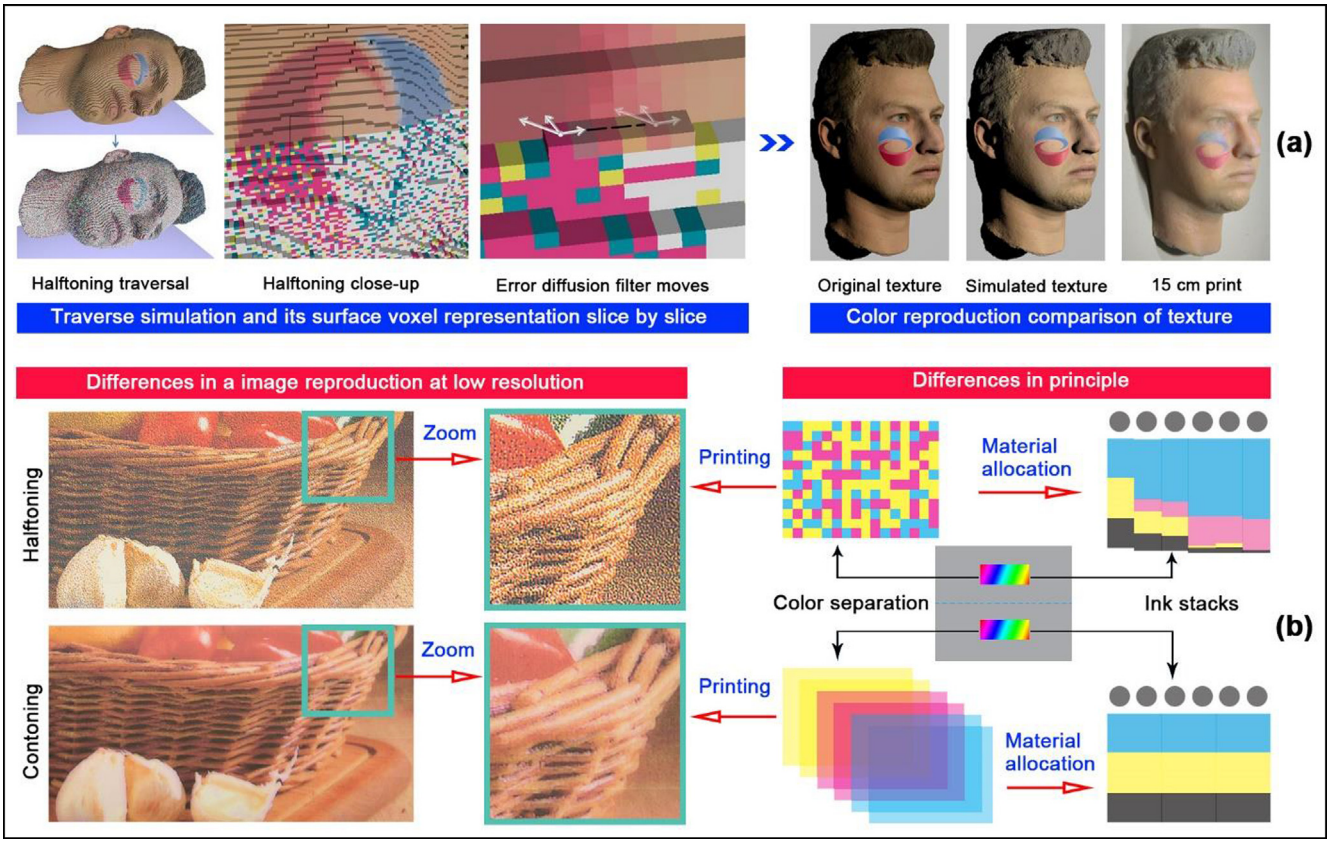

Fig. 8. Voxel unit generation: **(a)** halftoning printing; **(b)** contoning printing; Examples used with permission from [98], copyright (2015) ACM; [102], copyright (2017) ACM.

However, before describing voxel unit printing, three major challenges need to be addressed: the accurate generation of voxel droplets, the precise prediction of the droplet jetting behavior and the arrangement of color concentrations.

Initially, based on scalable error diffusion algorithms in 2D printing, the Fraunhofer IGD (Institute for Computer Graphics Research in Darmstadt) developed a novel traversal algorithm for solid voxelization to achieve full-color visualization with multi-jetting 3D printers [98,99]. The left part of Fig. 8 **(a)** shows a halftoning traversal simulation and details of the slice-wise voxelized surface, and its right part compares facial texture reproduction from their software simulation and color 3D print. The reproduction of each color on the texture is preserved, but differences in visual perception of the current overall appearance are still perceptible. Subsequently, this adaptive error diffusion halftoning approach has been further standardized for the RGBA (Red Green Blue Alpha) data format to control color layers of 3D color objects [100]. With general multi-material jetting 3D printers, color is represented discretely by ink drops at voxel positions. For instance, the GrabCAD Voxel 3D Printers launched by Stratasys in 2017 showed the *trans*-scale 3D printing at voxel level and image-based texture reproduction for transparent 3D entities [101]. Soon afterwards, the MIT CSAIL Computational Fabrication Group proposed a new contoning printing method based on spectral vector error diffusion algorithm to solve the layout discretization and color quantization issues in the resin-based 3D printing process [102].

Vividly, the differences between halftoning and contoning (continuous toning) for a voxel unit generation are illustrated in Fig. 8 **(b)**. The left part of Fig. 8 **(b)** exhibits an image printed at 180 dpi printer resolution, showing the outcomes of the halftoning (top) and contoning (bottom) methods, with no signs of spatial subsampling or unacceptable dot patterns in the contoning image. The reason for this behavior is that in a contoning image every pixel is printed with its individual tone whereas in an halftoning image, different color tones are generated by areas of different sizes covered by the same single color. Then in 2018, the Wyss Institute for Biologically Inspired Engineering at Harvard University and the MIT Media Lab's Mediated Matter Group developed a simple multi-material transformed voxel printing method by converting discontinuous data sets into dithered deposition marks for more accurate color reproduction with four cases [103]. This method focuses on preventing data alteration and boundary information loss for the color transition from a digital representation to the physical material compositions in a multi-material jetting process. Theoretically, given concise and computational spectral absorption, a weighted regression prediction model can be set up for arbitrarily many resin-based colorants and can further be extended to a color reproduction accuracy evaluation method for current all plastic-based color 3D printing processes.

However, one of the biggest limitations is that voxel colorization in plastic-based full-color 3D printing is achieved by the direct accumulation of only liquid droplets without further active materials, while a second material with a different physical form is used in paper- and powder-based full-color 3D printing. For this reason, the voxelized droplet coloring suffers the unpredictable hydrodynamics in the penetration or immersion of solid substrates (paper sheets, powder particles). More experimental studies are needed to understand and manage the voxel droplet jetting.

3. Color accuracy issues of full-color 3D printing techniques

To judge whether a universal accurate color reproduction framework can be derived for the full-color 3D printing methods

Table 1
A summary of color reproduction methods and their main features.

Studies	Color reproduction categories	Process principles	Materials	Specimen Geometry
Théo et al. (2017, 2018)	Optical parameter modeling	MJ	Plastic-based	Color patches
Elek et al. (2017)	Optical parameter modeling	MJ	Plastic-based	Color blocks
Sumin et al. (2019)	Optical parameter modeling	MJ	Plastic-based	Earth model
Song et al. (2013)	Optical parameter modeling	ME	Plastic-based	Color sphere
Rouiller et al. (2013)	Optical parameter modeling	VPPM, BJ	Plastic-based, powder-based	Cylinder, spot domes
Cheydleur. (2016)	Optical parameter modeling	VPPM	Plastic-based	Spot basketball
James. (2016)	Optical parameter modeling	MJ	Plastic-based	Cubes
Vu et al. (2016)	Optical parameter modeling	MJ	Plastic-based	Texture-less samples
Stopp et al. (2008)	Colorimetric difference evaluating	BJ	Powder-based	Cubes
Page et al. (2017)	Colorimetric difference evaluating	MJ	Plastic-based	Colored bands
Stanic et al. (2008)	Colorimetric difference evaluating	BJ	Powder-based	Color patches
Xiao et al. (2013a, 2013b, 2014)	Colorimetric difference evaluating	VPPM	Plastic-based	Soft tissue prostheses
Sohaib et al. (2018)	Colorimetric difference evaluating	BJ	Powder-based	Facial prostheses
Yuan et al. (2016a)	Colorimetric difference evaluating	SL	Paper-based	Hemispheres, cone
Yuan et al. (2016b, 2017a, 2017b)	Colorimetric difference evaluating	SL	Paper-based	Banana, container, medical models
Yuan et al. (2019, 2020)	Colorimetric difference evaluating	MJ	Plastic-based	Oil painting, 3D chart
Yan et al. (2018)	Colorimetric difference evaluating	SL	Paper-based	Geographical model
Chen et al. (2016)	Colorimetric difference evaluating	MJ	Plastic-based	Oil paintings
Sun et al. (2015, 2016)	Colorimetric difference evaluating	BJ	Powder-based	Color charts
Pi et al. (2016)	Colorimetric difference evaluating	BJ	Powder-based	Santa model
Li et al. (2016)	Colorimetric difference evaluating	SL	Paper-based	Color patches
Wei et al. (2018)	Colorimetric difference evaluating	ME	Plastic-based	Colored cloth
Michael et al. (2016)	Colorimetric difference evaluating	MJ	Plastic-based	Wall ornaments
Parraman et al. (2018)	Colorimetric difference evaluating	MJ	Plastic-based	Personalized map
Christoph et al. (2016)	Colorimetric difference evaluating	MJ	Plastic-based	Medical models
Zhang et al. (2015)	Computer-aided colorization	CHP	Plastic-based	Stanford rabbit
Schuller et al. (2016)	Computer-aided colorization	CTP	Plastic-based	Plutus cat
Muntoni et al. (2018)	Computer-aided colorization	ME	Plastic-based	Fertility, Kitten, Chinese Lion
Yuan et al. (2017c)	Computer-aided colorization	SL	Paper-based	Hollowing structures, cylinder
Wang et al. (2019)	Computer-aided colorization	BJ	Powder-based	Cuboid, cubes
Yang et al. (2018)	Computer-aided colorization	ME	Plastic-based	Colorful cupcake, bottle
Skylar-Scott et al. (2019)	Computer-aided colorization	ME	Plastic-based	Colorful cubes
Brunton et al. (2015)	Voxel droplet jetting	MJ	Plastic-based	Bald head, Ruslan, Nefertiti, Apple
Alan et al. (2018)	Voxel droplet jetting	MJ	Plastic-based	Anatomy model, lion, lizard
Urban et al. (2019)	Voxel droplet jetting	MJ	Plastic-based	Buddha, Stanford's dragon, Lucy model
Vahid et al. (2017)	Voxel droplet jetting	MJ	Plastic-based	Colorful mask, fish
Christoph et al. (2018)	Voxel droplet jetting	MJ	Plastic-based	Statue, patient hand

Table 2
A summary of pivotal accuracy issues and details from the studies.

Color reproduction categories	Studies	Printing material categories	Accuracy issues	Suitability Index
Optical parameter modeling	[43–46,51,52,59,60,61,62,63,64]	Plastic-based, powder-based	Acquisition issues	★★★☆
Colorimetric difference evaluating	[67,68,69–72,73–77,78–80,81–83,86,87,88]	Plastic-based, powder-based, paper-based	Acquisition issues, coloring issues	★★☆
Computer-aided colorization	[91,92,93,94,95,96,97]	Plastic-based, paper-based, powder-based	Coloring issues, rendering issues	★★★★
Voxel droplet jetting	[98,99,100,101,102,103]	Plastic-based	Rendering issues	★★★

mentioned above, the literature on various color 3D printing techniques is categorized in Table 1. This table contains most of the principles seen in full-color 3D printing together with commonly used materials, and represents the state of the art in color reproduction. For each color reproduction category, Table 2 exhibits relative subjective scale on the suitability for the universal color accuracy reproduction ranging from low (☆) to high (★★★★★). Herein, one hollow marker has the same weight as half a solid marker. For each category, the core accuracy issues are also correlated with current respective experimental studies.

Table 1 shows the principle statistical characteristics of the color 3D printing processes used in the four types of color reproduction methods, where the highest frequency is explored in MJ, followed by BJ, SL, ME and VPPM in that order. From the distribution of printing materials, plastic-based types are explored in the first place, followed by powder-based types, and finally by paper-based types. From the geometric characteristics of the prints, all kinds of geometric shapes are involved, and their surface color characteristics are also very complex. Overall, MJ, BJ, and ME have multiple types of color reproduction methods discussed above, but SL and VPPM have fewer types of color reproduction methods for current full-color 3D printing processes.

In Table 2, the three key issues affecting the accuracy of color reproduction in full-color 3D printing can be found in the research literature of colorimetric difference evaluating and computer-aided colorization, which both focus on two major types of color accuracy issues, while the other methods are limited to one type of color accuracy study. In terms of the printing material categories on which the color reproduction methods are based, the research literature of colorimetric difference evaluating and computer-aided colorization both covers the mainstream coloring materials, but there are minor differences in other color reproduction methods. The research literature of optical parameter modeling method focuses on plastic-based and powder-based color 3D printing processes, but its research on the optimization of color reproduction in paper-based full-color 3D printing is currently in a gap. The suit-

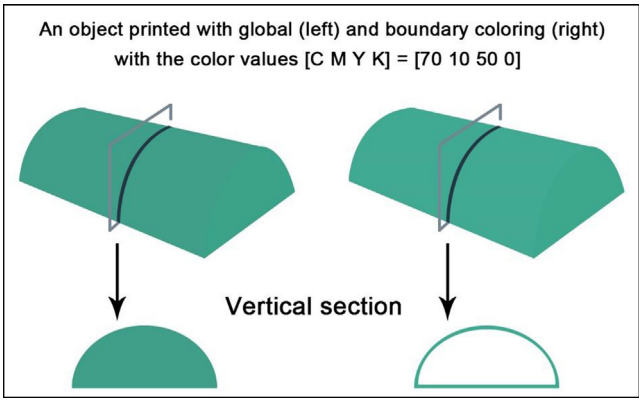

Fig. 9. The two coloring modes of the coloring phase: global coloring, left; boundary coloring, right.

ability index statistics show that current four categories of color reproduction methods vary in the development of a generic color accurate reproduction framework for full-color 3D printing and that there is the greatest potential to achieve this goal using computer-aided colorization.

Color reproduction is standardized in 2D printing and has similarities with the full-color 3D printing. To obtain accurate color reproductions for printed color images, one needs to understand the color transmission process. The color reproduction theory, a color quality evaluation framework and a color management system can contribute to the numerical models for faithful color reproduction. This has been standardized for 2D printing techniques over the past years. The academic community is aware that color reproduction behaves in 3D printing is distinct from in 2D printing, and its intrinsic differences in the color transmission flow are not studied and understood in depth. The "standardization" in this manuscript is to express how to enhance the color reproduction consistency of full-color 3D printing using different printing materials. Therefore, the coloring, rendering and acquisition issues for accurate full-color 3D printing are analyzed in detail.

3.1. Coloring issues of full-color 3D printing processes

In current full-color 3D printing, surface color information of printed object can be determined while its interior color is hard to detect and usually ignored. There are two ways to generate the outer surface color slice by slice: The first one is global coloring where each slice or layer is completely colored by the surface color. The second one is boundary coloring where each slice is only colored within some boundary layer of a certain thickness. These two modes are shown in Fig. 9.

In 2D printing, the color thickness is determined by the primary ink. In 3D printing, however, the thickness of the colored boundary region can vary. Essentially, the printing substrate and the thickness of the colored boundary layer determine the color reproduction accuracy. The full-color 3D printing substrate usually consists of the coloring material and the filling material in boundary coloring mode. The choice of an opaque and white filling substrate is more concise and efficient for the assignment of the ratio between the coloring material and the filling material in each color layer. However, the filling material in UV curable 3D printing can be either transparent or white UV ink, although this makes color prediction more difficult. In addition, optical properties of these achromatic substrates also affect the boundary colorization range. However, the effects of layer thicknesses and slicing strategies on the colored boundary region are not addressed completely. Further, when fixing the layer thickness, stacking the primary inks at the desirable boundary is also a new area to explore.

3.2. Rendering issues of full-color 3D printing processes

Printing substrates and coloring materials in full-color 3D printing differ from conventional 2D printing where paper or plastic sheets are used as printing substrates. There is specific research on how paper properties affect the color accuracy in 2D printing [104]. Currently, printed paper can easily be measured and analyzed. For example, 2D printing service providers can purchase tons of customized printing papers with consistent properties and almost no deviations in their thickness. However, in color 3D printing, every slice has a different slice underneath. Therefore, whiteness, transparency, smoothness, and glossiness vary from one layer to the next and moreover depend on all slices' underneath. This dependency on the layer's underneath is a main problem in accurate color reproduction and has not been addressed so far. Furthermore, it is crucial to quantify the effect of substrate thickness on surface characteristics by the measured density or spectral values [105]. In addition, properties of layers need to be matched with the underlying layer substrates. The way in which the colored printing substrate is deposited and attaches to the upside of the slice underneath is markedly different from 2D printing. The rendering principles of 2D printing are depicted in Fig. 10.

In 2D printing on paper or film, the paper or film is regarded as the printing substrates, and color ink consisting of specific discrete ink droplets is applied with a fixed thickness. The color reproduction accuracy is determined by the ink dot area coverage on the paper surface. In the example shown in Fig. 10 **(a)** & **(b)**, the magenta droplets with a thickness σ are evenly distributed on the paper covering half the area. This is fundamentally different in full-color 3D printing. In an analogous example shown in Fig. 10 **(c)** & **(d)**, the magenta dots cover a boundary layer of width L of each slice with thickness H and lie on a regular 3D grid. However, they are irregularly positioned and spaced on the boundary. Therefore, halftone screening techniques perform poorly in 3D printing. The area without magenta droplets is covered by achromatic material such as UV cured white adhesive, which also influences the final color, its brightness and saturation.

3.3. Acquisition issues for full-color 3D printing

In full-color 3D printing, the input is a 3D data file while the output is a colored 3D entity. Color measuring devices used in 2D printing do not work for arbitrary surfaces in general. Typically, different reflectance values can be perceived at different points on a general surface with the same viewing and illumination angle. In addition, it is also illustrated that the measured colorimetric values are not constant for a fixed point on the curved surface in Fig. 3 **(c)**, when changing either the number of illuminates used or their angles relative to the surface. Worldwide, the color 3D printing industry is investigating these theoretical and practical issues with color 3D scanners as discussed in Section 2.1. In an example shown in Fig. 11 **(a)**, a customized wine package with a green brand logo is completely printed by a powder-based color 3D printer. The red dashed circle marks a tiny complex curved surface on the green logo that easily leads to poor color reproduction and acquisition.

Besides the specialized optical measuring instruments described together with Fig. 4, there are other color 3D scanners employed that use high-definition cameras for shape and surface texture acquisition [78,106]. To explain why poor acquisition performance occurs with such camera-based scanners, a half-cylinder model that approximates the geometry sampled in the red circle is considered as an example shown in Fig. 11 **(b)**. In a camera image of it, distances are not preserved, which leads to a mismatch of points on the color 3D object. Further, non-orthogonal projections (as by a camera) are non-area preserving and lead to inaccurate color acquisitions. To reduce these accuracy problems, it appears

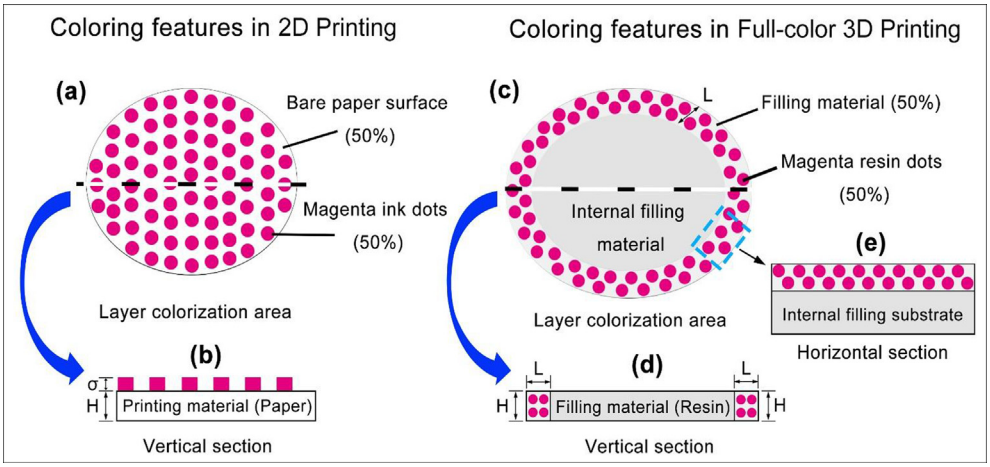

Fig. 10. The color rendering principles in 2D printing and powered-based full-color 3D printing: **(a)** a colorization area in 2D printing; **(b)** a vertical section of **(a)**; **(c)** a colorization area in full-color 3D printing; **(d)** a vertical section in full-color 3D printing; **(e)** a horizontal section in full-color 3D printing.

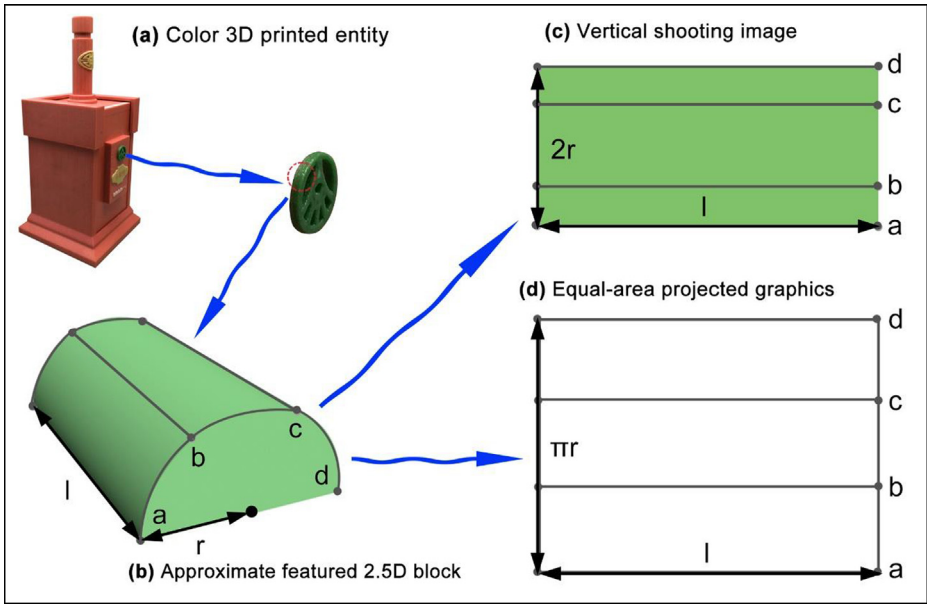

Fig. 11. An example illustrating the accuracy challenge of color acquisition for color 3D prints: **(a)** a color 3D printed entity with a specific green brand logo; **(b)** a 2.5D approximation of the area circled in red on the printed logo; **(c)** a conventional global photography in vertical direction of **(b)**; **(d)** an area preserving projection of **(b)**.

therefore possible to measure key color features with an area preserving transformation based on photography in normal direction and match image points to points on the 3D printed entities, rather than on some planes that are commonly used in the additive manufacturing community. Furthermore, efficient segmentations into regions with key features and their projections are essential to accurately capture curved surfaces. For example, Fig. 11 **(c)** gives a photographic image where the colors match exactly but the positions do not match one by one, while the map used in Fig. 11 **(d)** is area preserving and one to one, but the colors do not match exactly. Combing two such maps to solve the twofold matching is a problem in itself. It should be explained that the Fig. 11 **(c)** is a stitching of multiple vertical shots and therefore has no shadows.

4. Outlook on an accurate color reproduction framework

The workflow of 3D printing generally consists of three parts: the 3D model input, the layer construction and the material arrangement. Full-color 3D printing is where the importance of color is more emphasized in this workflow.

To begin with a 3D model with a simple texture, the raw material for the color is just roughly selected, rather than laboriously determined. For full-color 3D printing, 3D models with complex textures must be converted into the OBJ or VRML format. These two formats contain RGB color information for texture visualization, which sometimes leads to color deviations or tone value compressions. Since the color range of a 3D model in the usual sRGB color space is often larger than that of the coloring materials in full-color 3D printing, an additional color management is essential for accurate color reproduction. In 2D printing, the color management has been standardized using ICC profiles, which provides the desired gamut mapping strategies and algorithms in the standard conversion module [107].

However, for accurate full-color 3D printing, color management is still new. In Reference [98], Brunton et al. explore a halftoning framework for faithfully 3D printed color objects. Although designed for polymer-based color 3D printing with translucent

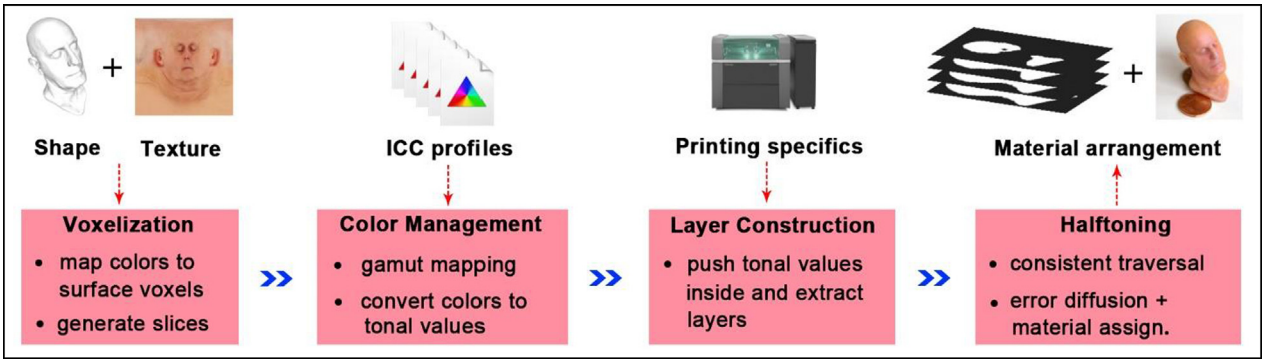

Fig. 12. A color 3D printing workflow for halftoning framework. Examples used with permission from [98], copyright (2015) ACM.

printing materials, their framework can potentially be extended to other material types with the following elements and optimizations of the four core steps illustrated in Fig. 12: voxelization, color management, layer construction, and material arrangement.

In the voxelization step: the color texture has to be mapped to the surface voxels and slices with voxels of the same z-coordinates have to be generated from. Voxelization is the conversion of 3D model data into voxel data, either from a mesh model or a point cloud model [108,109]. The voxel data can also be divided into surface voxel and internal voxel depending on its position in the 3D model. The voxel implementation algorithms can be divided into two categories: CPU (central processing unit) method and GPU (graphics processing unit) method [110,111]. Then, surface voxels associated with RGBA values are to generate slices with specific strategies. However, the thickness limitations of printing substrates can also affect voxel unit output. For example, the thickness of paper sheets used in paper-based full-color 3D printing is normally 104 μm, and the thickness of powder substrates in powder-based full-color 3D printing is generally 100 μm, which is far from the fine resolution used in plastic-based full-color 3D printing. Further experiments are needed before color halftoning can be extended to coarser resolutions. The approach taken in the color similarity perception analysis for customized 3D tablets can, for example, serve as a reference for such experiments [112].

The color management step includes a gamut mapping and color separation. Gamut mapping means to map color data to the printer's tonal values based on the ICC profiles or iccMax profiles [30,61,107]. Since there are more than 100 different 3D printing equipment types, the gamut mapping, which depends on the printing material, is complex [113]. The ICC provides just four rendering intentions, but there are many more color gamut mapping algorithms ranging from a pointwise gamut mapping to a spatial gamut mapping, as well as from small to large color gamuts [114–116]. However, all these traditional gamut mapping algorithms are not perfect for full-color 3D printing. As convolutional neural networks (CNN) have already been applied to the color gamut mapping of ultra-high-definition television image [117], it is conceivable that machine learning could help to find suitable gamut mappings for full-color 3D printing systems.

Currently, despite the iccMax profile's superiority in expressing material appearance parameters, its encapsulated BRDF parametric module is not promoted by the ICC [61]. It is difficult to develop an advanced material appearance model because they need more data space, lead to longer conversion times, and because the conversion of appearance and color parameters between different iccMax profiles is not standardized.

Accordingly, color separation then means to map tonal values to the primary colors represented by printing materials (coloring materials and filling materials). The primary colors for full-color 3D printing are cyan (C), magenta (M), yellow (Y), black (K), and white (W), even some devices are available in spot colors such as orange. In principle, there are only two options for color separation: halftoning (discrete color printing) and contoning (continuous color printing). Current halftoning techniques consist of dithering, error diffusion, and iterative methods [118]. As explained in Section 2.4, the contoning method can provide more faithful reproduction, depending on an accurate spectral function match of each color layer. This is closely related to the computational assignment of the coloring materials (inks, binders or curing resins) and is further discussed below with the material arrangement step.

For the layer construction step, most full-color 3D printing systems are equipped with a dedicated slicing tool to better accommodate the color representation of specific printing materials. Ordinary 3D printing systems only need to consider the number and thickness of the layers, but full-color 3D printing systems still need to determine the boundary coloring width of each slice. However, the current color width of each layer is directly fixed in the slicing software with a default value that cannot be modified by the user during the printing process. The boundary coloring width is easily understood and implemented for the plastic-based 3D printing techniques using the same physical state of coloring resins and filling resins, such as stereo lithography (SLA), digital lithography projection (DLP), continuous liquid interface production (CLIP), continuous inkjet printing (CIJ) and drop-on-demand inkjet printing (DOD) [119]. However, beyond that, few systematic studies have been conducted to investigate the effect of the boundary coloring width on color reproduction accuracy in the layer construction. In fact, in our previous studies on accurate reproduction of 2.5D oil paintings, it was also found that the printing sequence of color and non-color layers significantly affects the color reproduction accuracy by the reduction of nasty jagged effect [78,120]. Recently, a unique 3D color test chart was purposefully designed to examine the effect of colored layer features on color reproduction of plastic- and paper-based 3D printed parts and the results also revealed a significant correlation based on image quality metrics from the HD orthographic imaging, but these didn't show a linear quantization trend [121,122]. To determine the slicing strategy, the thickness, and number of sliced layers, it should be clearly understood how interior color tones influence the ones on the outer surface. In future, an intelligent regulation of the boundary coloring width based on the adaptive feedback algorithms can be embedded into non-polymer based full-color 3D printing systems.

Finally, the material arrangement step outputs slice files listing the specific components per voxel in a printer format. When the boundary color and computational width of each layer is determined, each digital color can be physically visualized by the assigned coloring and filling materials. The color separation

determines the primary material choice, but specific implementation methods depend on the boundary coloring width. For example, Brunton et al. [98] and Babaei et al. [102] discussed two spectral function predictions for the boundary coloring width to optimize the material arrangement within their halftoning and contoning framework, respectively.

In 3D halftoning, any layer is filled at discrete spots with the coloring material by stacking a mixture of primary color droplets with variable concentrations and ratios [123]. In this framework, the number of primary colors and inks concentrations is quickly obtained. With contoning however, different tones are achieved by stacking colors with variable depths. This means that color spots end up with different thicknesses. It is tricky to determine a smallest sufficient number of spot categories based on the spectral reflectance in normal direction of the color layer rather than in its building direction. If the 3D contoning is performed only in the boundary coloring area of the printed layer, a boundary contoning framework can be formed to overcome the current material voxelization challenges of paper-based and powder-based full-color 3D printing. Besides, collotype printing [124] is a classical continuous-tone printing process for high-fidelity reproduction of 2D or 2.5D artworks. It requires extreme color separation skills to determine the spot color categories for an authentic reproduction of treasured Chinese brush paintings [125]. At present, these subjective color separation skills have not been fully implemented by objective digital techniques. If these challenges can be mastered together, the contoning framework will also be applicable to a precise color control for powder- and paper-based full-color 3D printing.

In summary, the evolution from boundary coloring mode to boundary coloring theory is an important reference for the implementation and optimization of the current color accurate reproduction framework for full-color 3D printing, accompanied by the construction of the boundary coloring width computational model. When the boundary coloring theory and the boundary coloring width model are standardized, the boundary contoning framework can be coded for the voxel arrangement of various printing substrates. Moreover, this will fundamentally change the current theories for accurate color reproduction and quality evaluation in full-color 3D printing. Furthermore, the development of surface coloring efficiency prediction models based on mainstream color 3D printers and existing printing materials can improve the suitability of generic boundary coloring width models for accurate color reproduction in various full-color 3D printing processes.

5. Conclusion

This review paper gives an overview over the four predominant color reproduction methods in Section 2 and a summary of the state of the art in full-color 3D printing. Current studies on accurate color reproduction for color 3D printing focus mainly on MJ, BJ, SL and ME, all of which are also familiar to the materials & design community. However, coloring, rendering, and acquisition issues are not comprehensively investigated and are challenging problems in developing a general color accuracy evaluation system for full-color 3D printing.

Color accuracy problems and potential solutions are discussed with vivid illustrations and easy-to-understand subtitles. Computer-aided coloring methods show the greatest potential for achieving accurate full-color 3D printing with many types of printing materials. Based on the halftoning and contoning techniques to generate voxel units in plastic-based full-color 3D printing, a comprehensive outlook on the implementation of an accurate color reproduction framework with four core steps is provided and further extended to other physical states of printing materials. Combining the boundary contoning theory and the surface coloring efficiency prediction model can inspire interested scholars to rethink and develop powerful coloring materials to precisely modulate computational material assignment for a generic accurate color reproduction framework. Besides, test benchmark design, experimental guidelines and numerical analysis models for evaluating the color reproduction performance of full-color 3D printing are also key to implementing accurate material-aware full-color 3D printing. Furthermore, the accurate full-color 3D printing processes can also be extended to full-color 4D printing with precise color response, which is also a new research area for scholars in the field of functional material design.

Funding

This work has been financially supported by the Natural Science Foundation of China (Grant No. 61973127), Guangdong Provincial Science and Technology Program (Grant No. 2017B090901064), and Chaozhou Science and Technology Program (Grant No. 2020ZX14).

Declaration of Competing Interest

The authors declare that they have no known competing financial interests or personal relationships that could have appeared to influence the work reported in this paper.

References

[1] J.N. Fullerton, G.C. Frodsham, R.M. Day, 3D printing for the many, not the few, Nat. Biotech. 32 (11) (2014) 1086–1087.
[2] Wohlers Report 2017, http://www.wohlersassociates.com/2017report.htm. ISBN: 978-0-9913332-3-3.
[3] Amit Bandyopadhyay, Kellen D. Traxel, Invited Review Article: Metal-Additive Manufacturing — Modeling Strategies for Application-Optimized Designs, Addit. Manuf. 22 (2018) 758–774.
[4] L. Safai, J.S. Cuellar, G. Smit, A.A. Zadpoor, A review of the fatigue behavior of 3D printed polymers, Addit. Manuf. 28 (2019) 87–97.
[5] W. Elkhuizen, T. Essers, Y. Song, J. Geraedts, C. Weijkamp, J. Dik, S. Pont, Gloss, Color, and Topography Scanning for Reproducing a Painting's Appearance Using 3D Printing [J], ACM J. Comput. Cult. He. 12 (4) (2019) 1–22.
[6] L. Ren, Z. Song, H. Liu, et al., 3D printing of materials with spatially nonlinearly varying properties [J], Mater. Design 156 (OCT.) (2018) 470–479.
[7] Y.L. Cheng, C.H. Chang, C. Kuo, Experimental study on leveling mechanism for material-jetting-type color 3D printing, Rapid Prototyp. J. 26 (1) (2020) 11–20.
[8] 3D-SYSTEMS. 2014. ProJet 860Pro. http://www.3dsystems.com/3dprinters/professional/projet-860pro (accessed May 2021).
[9] MCOR TECHNOLOGIES. 2014. MCOCR IRIS. http://MCORtechnologies.com/3d-printers/iris/ (accessed May 2021).
[10] STRATASYS. 2014. Objet500 Connex3. http://www.stratasys.com/3dprinters/production-series/connex3-systems (accessed May 2021).
[11] ISO/ASTM 52900, Additive manufacturing—general principles—requirements for purchased AM parts 2015.
[12] M.J. Tsai, C.W. Mei, Y.L. Cheng, et al., in: International Conference on Machine Learning and Cybernetics (ICMLC), 2017, pp. 664–669.
[13] M.R. León, M. Umorin, M. Özcan, et al. Color dimensions of additive manufactured interim restorative dental material [J]. J. Prosthetic. Dent, 2019.
[14] L. Zhou, J. Fu, Y. He, A review of 3D printing technologies for soft polymer materials, Adv. Funct. Mater. 2000187 (1–38) (2020), https://doi.org/10.1002/adfm.202000187.
[15] T. Tran, On the Bottleneck of Adopting 3D Printing in Manufacturing, Virtual and Physical Prototyping 12 (4) (2017) 333–334.
[16] T. Kuipers, W. Elkhuizen, J. Verlinden, et al., Hatching for 3D prints: Line-based halftoning for dual extrusion fused deposition modeling[J], Comput. Graph-UK 74 (2018) 23–32.
[17] X.C. Wang, C. Chen, J.P. Yuan, G.X. Chen, Color Reproduction Accuracy Promotion of 3D-Printed Surfaces Based on Microscopic Image Analysis, Int J Pattern. Recogn. 34 (01) (2020) 5593–5600.
[18] H.C. Wu, T.C.T. Chen, Quality control issues in 3D-printing manufacturing: a review[J], Rapid Prototyp. J. 24 (3) (2018) 607–614.
[19] M. Amini, S. Chang, Process monitoring of 3D metal printing in industrial scale[C]//ASME 2018 13th International Manufacturing Science and Engineering Conference, American Society of Mechanical Engineers Digital Collection (2018).

[20] J.Y. Lee, A.P. Nagalingam, S.H. Yeo, A Review on the State-of-the-art of Surface Finishing Processes and Related ISO/ASTM Standards for Metal Additive Manufactured Components, Virtual and Physical Prototyping (2020) 1–29.
[21] G.X. Chen, C. Chen, Z.H. Yu, H. Yin, L.X. He, J.P. Yuan, Color 3D Printing: Theory, Method, and Application. New Trends in 3D Printing, IntechOpen (2016) d), https://doi.org/10.5772/63944.
[22] Intechopen company (2016). https://www.intechopen.com/ books/new-trends-in-3d-printing (accessed May 2021).
[23] ICC, Taipei, 2016. "Color Management in Displays and 3D Printing". http://www.color.org/events/taipei/1-ICC_overview.pdf (accessed May 2021).
[24] I. Tastl, M. A. Lopez-Alvarez, A. Ju, et al. A Soft-proofing Workflow for Color 3D Printing - Addressing Needs for the Future[J]. J. Electron. Imaging, 2019, 2019 (6):479-1-479-6.
[25] J.P. Yuan, C. Chen, J.N. Tian, D.Y. Yao, H. Li, G.X. Chen, Color Reproduction Evaluation of Paper-Based Full-Color 3D Printing Based on Image Quality Metrics, Digital Printing 5 (2020) 26–34.
[26] G.X. Chen, X.C. Wang, H.Z. Chen, C. Chen, Realization of Rapid Large-Size 3D Printing Based on Full-Color Powder-Based 3DP Technique, Molecules 25 (2020) 2037.
[27] J.P. Yuan, M. Zhu, B.H. Xu, G.X. Chen, Review on processes and color quality evaluation of color 3D printing, Rapid Prototyp. J. 24 (2) (2018) 409–415.
[28] H.R. Kang, 1993, January. Comparisons of color mixing theories for use in electronic printing. In Color and Imaging Conference, Society for Imaging Science and Technology, 1993, (1), 78-82.
[29] X. Lin, M. Wiertlewski, Sensing the frictional state of a robotic skin via subtractive color mixing, IEEE Rob. Autom. Lett. 4 (3) (2019) 2386–2392.
[30] ICC. 2010. File Format for Color Profiles, 4.3.0.0 edition. http://www.color.org. (accessed May 2021).
[31] G.X. Chen, Advances in 3D Printing Research / 2016–2017 Sensorimaging Disciplinary Development Report / CCSA Disciplinary Development Research Series [M], China Science and Technology Press, Beijing, 2018, pp. 283–302.
[32] CIE, CIE Tutorial on Colorimetry and Visual Appearance http://cie.co.at/news/cie-tutorials-colorimetry-and-visual-appearance (2017). (accessed May 2021).
[33] R. Cheydleur, Measurement For 3D Printing. ICC Display & 3D Print Meeting proceedings, Taipei (2016).
[34] Proc. SPIE 9398, Measuring, Modeling, and Reproducing Material Appearance 2015, 939801 (15 April 2015), Soci. for Imaging. Sci. & Technol.; doi: 10.1117/12.2193203.
[35] Appearance Printing European Advanced Research School, 2017. http://www.appears-itn.eu/ (accessed May 2021).
[36] H. Kim, Y. Lin, T.L.B. Tseng, A review on quality control in additive manufacturing, Rapid Prototyp. J. 24 (3) (2018) 645–669.
[37] S. Tominaga, R. Schettini, A. Trémeau, T. Horiuchi, Computational Color Imaging, 7th International Workshop, CCIW 2019, Chiba, Japan, March 27-29, 2019, https://link.springer.com/book/10.1007/978-3-030-13940-7 (accessed May 2021).
[38] H.C. Hottel, A.F. Sarofim, Radiative transfer, Landolt-Börnstein -Group VI Astronomy and Astrophysics 142 (9) (1967) 42–44.
[39] R.E Hummel. Optical Properties of Materials. In: Understanding Materials Science. Springer, New York, USA, 2004. https://doi.org/10.1007/0-387-26691-7_13.
[40] J. Wang, S. Zhao, X. Tong, et al., Modeling and Rendering of Heterogeneous Translucent Materials Using the Diffusion Equation, ACM Trans. Graph. 27 (1) (2008) 1–18.
[41] D.R., Ney and E.K. Fishman, "Volumetric Rendering." IEEE Computer Graphics & Applications 10.2(1990):24-32.
[42] A. Genty-Vincent, T.P.V. Song, C. Andraud, M. Menu, Four-flux model of the light scattering in porous varnish and paint layers: towards understanding the visual appearance of altered blanched easel oil paintings, Appl. Phys. A 123 (7) (2017) 473.
[43] T.P.V. Song, C. Andraud, M.V.O. Segovia, Towards Spectral Prediction of 2.5D Prints for Soft-Proofing Applications, International Conference on Image Processing Theory Tools & Applications, 2017.
[44] T.P.V. Song, C. Andraud, M.V.O. Segovia, Spectral predictions of rough ink layers using a four-flux model, Twenty Fifth Color and Imaging Conference (2017).
[45] T.P.V. Song, C. Andraud, L.R. Sapaico, M.V.O. Segovia, Color prediction based on individual characterizations of ink layers and print support, Conference: IS&T International Symposium on Electronic Imaging 2018, Material Appearance, 2018.
[46] T.P.V. Song. Optical models for appearance management of printed materials. Centre de Recherche et Restauration des Musées de France. PhD thesis, 2018.
[47] T.F. Schiff, J.C. Stover, D.R. Cheever, D. R. Bjork, Maximum and minimum limitations imposed on BSDF measurements. Proceedings of SPIE - The International Society for Optical Engineering, 1989, 66.
[48] C. Asmail, Bidirectional scattering distribution function (BSDF): a systematized bibliography, J. Res. Nat. Inst. Stand. Technol. 96 (2) (1991).
[49] G.V.G. Baranoski, A. Krishnaswamy, "Light, Optics, and Appearance", in Light & Skin, Interactions (2010).
[50] E. Eon, G.A. Irving, Quantized-Diffusion Model for Rendering Translucent Materials. ACM Trans. Graph., 30, 4, Article 56 (July 2011), 13 pages. DOI: 10.1145/1964921.1964951.
[51] O. Elek, D. Sumin, R. Zhang, T. Weyrich, K. Myszkowski, B. Bickel, A. Wilkie, J. Křivánek. Scattering-aware Texture Reproduction for 3D Printing. ACM Trans. Graph. 36, 6, Article 241 (November 2017), 15 pages.
[52] D. Sumin, T. Rittig, V. Babaei, T. Nindel, A. Wilkie, P. Didyk, B. Bickel, J. Křivánek, K. Myszkowski, T. Weyrich, Geometry-Aware Scattering Compensation for 3D Printing. ACM Trans. Graph. 38, 4, Article 111 (July 2019), 14 pages.
[53] B.T. Phong, Illumination for computer generated pictures, Commun. ACM 18 (6) (1975) 311–317.
[54] G.J. Ward, Measuring and modeling anisotropic reflection, ACM Computer Graphics (ACM) 26 (2) (1992) 265–272.
[55] S.R. Marschner, S.H. Westin, E.P.F. Lafortune, K.E. Torrance, D.P. Greenberg, Image-based BRDF measurement including human skin. In: Lischinski D., Larson G.W. (eds) Rendering Techniques' 99. Eurographics. Springer, Vienna. (1999).
[56] D.B. Goldman, B. Curless, A. Hertzmann, S.M. Seitz, in: Shape and spatially-varying BRDFs from photometric stereo, IEEE, Piscataway, NJ, 2005, pp. 341–348.
[57] O. Rouiller, B. Bickel, J. Kautz, W. Matusik and M. Alexa, 3D-Printing Spatially Varying BRDFs. IEEE Comput. Graph & Appl. 33(6) (2013) 48-57. Nov.-Dec. 2013, doi: 10.1109/MCG.2013.82.
[58] M.M. Bagher, C. Soler, N. Holzschuch, Accurate fitting of measured reflectance using a Shifted Gamma micro-facet distribution. Computer Graphics Forum. Oxford, UK: Blackwell Publishing Ltd, 31(4) (2012) 1509-1518.
[59] L.N. Song, Research on Appearance Reproduction of Object Surface Based on Bidirectional Reflectance Distribution Function, Electro-Optic Technol. Appl. 28 (4) (2013) 10–15.
[60] L. Simonot, G. Obein, B. Bringier, D. Meneveaux, Modeling, measuring, and using BRDFs: significant French contributions, JOSA-A 36 (11) (2019) 40–50.
[61] V. James, 3D appearance management using iccMax, ICC Display & 3D Print Meeting proceedings, 2016.
[62] 3MF Consortium. 3D Manufacturing Format Specification and Reference Guide, 1 (2015) 1-48.
[63] B.M. Vu, P. Urban, T.M. Tanksale, S. Nakauchi, Visual perception of 3D printed translucent objects, Color and Imaging Conference. Soci. for Imaging. Sci. & Technol. 1 (2016) 94–99.
[64] W.S. Elkhuizen, T.T. Essers, Y. Song, S.C. Pont, J.M. Geraedts, J. Dik, Gloss Calibration and Gloss Gamut Mapping for Material Appearance Reproduction of Paintings, EUROGRAPHICS Workshop on Graphics and Cultural Heritage (2018) 161–164.
[65] S. Stopp, T. Wolff, F. Irlinger, T. Lueth, A new method for printer calibration and contour accuracy manufacturing with 3D print technology, Rapid Prototyp. J. 14 (3) (2008) 167–172.
[66] M. Page, G. Obein, C. Boust, A. Razet, Adapted Modulation Transfer Function Method for Characterization and Improvement of 3D printed surfaces, Elect. Imaging. 8 (2017) 92–100.
[67] M. Stanić, B. Lozo, T. Muck, S. Jamnicki, R. Kulčar, Color measurements of three-dimensional ink-jet prints, Proceedings of NIP, Pittsburgh 24 (2008) 6–11.
[68] M. Stanic, B. Lozo, D.G. Svetec, Colorimetric properties and stability of 3D prints, Rapid Prototyp. J. 18 (2) (2012) 120–128.
[69] K.D. Xiao, F. Zardawi, R. Noort, J.M. Yates, Color reproduction for advanced manufacture of soft tissue prostheses, J Dent. 41 (2013) 15–23.
[70] K.D. Xiao, F. Zardawi, R. Noort, J.M. Yates, Developing a 3D Colour Reproduction System for Additive Manufacturing of Facial Prostheses, Color and Imaging Conference. Soci. for Imaging. Sci. & Technol. 1 (2013) 206–209.
[71] K.D. Xiao, F. Zardawi, R. Noort, J.M. Yates, Developing a 3D color image reproduction system for additive manufacturing of facial prostheses, Int J of Adv. Manuf. Technol. 70 (2014) 2043–2049.
[72] A. Sohaib, K. Amano, K.D. Xiao, J.M. Yates, C. Whitford, S. Wuerger, Colour quality of facial prostheses in additive manufacturing, Int J of Adv. Manuf. Technol. 96 (1–4) (2018) 881–894.
[73] L.X. He, G.X. Chen, Effect of Aqueous Adhesives on Color of Paper Surface in Paper-based 3D Printing, Pack. Eng. 37 (3) (2016) 153–156.
[74] J.P. Yuan, G.X. Chen, Z.H. Yu, Speedup Method of paper-based 3D Color printing Based on Slicing strategies, Pack. J. 8 (1) (2016) 53–58.
[75] J.P. Yuan, G.X. Chen, J.H. Liao, Z.H. Yu, Visualization of Large-Size Model Based on Paper-Based 3D Printing, Advanced Graphic Communications, Pack. Eng. & Mater. 369 (2016) 333–338.
[76] J.P. Yuan, X.Y. Yan, X.C. Wang, G.X. Chen, Paper-based 3D printing industrialization for customized wine packaging applications, NIP & Digit. Fabric. Conf. 1 (2017) 118–121.
[77] X.Y. Yan, J.P. Yuan, G.X. Chen, Applications Analysis of Paper-Based Color 3D Printing in the Map Industry. In: Zhao P., Ouyang Y., Xu M., Yang L., Ren Y. (eds) Applied Sciences in Graphic Communication and Packaging. Lecture Notes in Electrical Engineering, 477 (2018) 377-383. Springer, Singapore. https://doi.org/10.1007/978-981-10-7629-9_46.
[78] C. Chen, 3D Digitalization and 3D Printing Reproduction Method for Oil Paintings, South China University of Technology, PhD Report, 2016.
[79] L.X. He, Study on Paper-based 3D Printing Based on DEM Data, South China University of Technology, Master Report, 2016.
[80] J.P. Yuan, L. Cai, X.C. Wang, G.X. Chen, Visualization of Biomedical Products based on Paper-based Color 3D Printing, NIP & Digit. Fabric. Conf. 1 (2019) 128–131.
[81] P.L. Sun, Y. Sie, Color dithering methods for LEGO-like 3D printing. Color Imaging XX: Displaying, Processing, Hardcopy, and Applications. Int Society for Opt. and Photo. 93950J (2015) 9395: 9399.
[82] P.L. Sun, Y.P. Sie, Color uniformity improvement for an inkjet color 3D printing system, Elect. Imaging 20 (2016) 1–6.

[83] Y.P. Pi, P.L. Sun, Color gamut mapping for 3D printing, ICC Display & 3D Print Meeting proceedings, 2016.
[84] Z.Y. Li, H. Min, G.H. Cui, H.X. Liu, Evaluation of the Color-difference Formulae for Neutral Colors. Advanced Graphic Communications, Pack. Tech. & Mater. (2016).
[85] CIE TC 8-17, Methods for Evaluating Color Difference between 3D Color Objects, http://www.cie.co.at/technical-work/jtcs. (2017). (accessed May 2021).
[86] C.A. Wei, X.X. Wan, J.F. Li, A modified single-constant Kubelka-Munk model for color prediction of pre-colored fiber blends, Cellulose 25 (6) (2018) 1–12.
[87] D. Michael, Elevated printing: application use cases, ICC Display & 3D Print Meeting proceedings, 2016.
[88] C. Parraman, M.V.O. Segovia, 2.5 D Printing: Bridging the gap between, 2D and 3D applications., John Wiley & Sons, 2018.
[89] B. Christoph, K. Dominik, J.C. Weaver, O. Neri, Data-Driven Material Modeling with Functional Advection for 3D Printing of Materially Heterogeneous Objects, 3D Print. Addit. Manuf. 3 (2) (2016) 71–79.
[90] Y.B. Dong, P.J. Li, Research on the modification of water transfer PVA sheet after adding starch, Appl. Chem. Industry 36 (4) (2007) 376–379.
[91] Y.Z. Zhang, C.J. Yin, C.X. Zheng, K. Zhou, Computational hydrographic printing, ACM Trans. Graph. 34 (4) (2015) 13–24.
[92] C. Schuller, D. Panozzo, A. Grundhofer, H. Zimmer, E. Sorkine, S.H. Olga, Computational thermoforming, ACM Trans. Graph. 35 (4) (2016) 43–52.
[93] A. Muntoni, M. Livesu, R. Scateni, A. Sheffer, D. Panozzo, Axis-Aligned Height-Field Block Decomposition of 3D Shapes, ACM Trans. Graph. 1 (1) (2018) 1–15.
[94] J.P. Yuan, Z.H. Yu, G.X. Chen, M. Zhu, Y.F. Gao, Large-size color models visualization under 3D paper-based printing, Rapid Prototyp. J. 23 (5) (2017) 911–918.
[95] J.P. Yuan, Y.M. Liu, G.X. Chen, L.X. He, Process Analysis of Seamless Adhesion for Cutting Model Printed by Color Paper-Based 3D Printing. Advanced Graphic Communications and Media Technologies. Lecture Notes, Electr. Eng. 417 (2017) 483–488.
[96] M.H. Yang, X.G. Lv, X.J. Liu, J.Q. Zhang, Research on color 3D printing based on color adherence, Rapid Prototyp. J. 24 (1) (2018) 37–45.
[97] M.A. Skylar-Scott, J. Mueller, C.W. Visser, J.A. Lewis, Voxelated soft matter via multimaterial multinozzle 3D printing, Nature 575 (7782) (2019) 330–335.
[98] A. Brunton, C.A. Arikan, P. Urban, Pushing the Limits of 3D Color Printing: Error Diffusion with Translucent Materials, ACM Trans. Graph. 35 (1) (2015) 1–13.
[99] B. Alan, A.A. Can, M.T. Tejas, P. Urban, 3D printing spatially varying color and translucency, ACM Trans. Graph. 37 (4) (2018) 157–170, https://doi.org/10.1145/3197517.3201349.
[100] P. Urban, T.M. Tanksale, A. Brunton, B.M. Vu, S. Nakauchi, Redefining A in RGBA: Towards a Standard for Graphical 3D Printing, ACM Trans. Graph. 1 (1) (2019) 1–15.
[101] Stratasys, GrabCAD, https://www.stratasys.com/software, (2017). (accessed May 2021).
[102] V. Babaei, K. Vidimče, M. Foshey, A. Kaspar, P. Didyk, W. Matusik, Color Contoning for 3D Printing, ACM Trans. Graph. 36 (4) (2017) 124–139.
[103] B. Christoph, K. Dominik, C.W. James, S. Sunanda, A. Hosny, J. Costa, N. Oxman, Making data matter: Voxel printing for the digital fabrication of data across scales and domains, Sci. Adv. 4 (5) (2018) eaas8652.
[104] O. Norberg, M. Andersson, B. Kruse, The influence of paper properties on color reproduction and color management, NIP & Digit. Fabric. Conf. 2 (2003) 836–840.
[105] A. Nadir, Effect of Layer Thickness on Surface Properties of 3D Printed Materials Produced from Wood Flour/PLA Filament, Polym. Test. 71 (2018) 163–166.
[106] P.C. Zhang, T.J. Arre, A. Ide-Ektessabi, A line scan camera-based structure from motion for high-resolution 3D reconstruction, J. Cult. Herit. 16 (5) (2015) 656–663.
[107] A. Sharma, Understanding color management, John Wiley & Sons, 2018.
[108] F. Liu, Voxelization processing method and device based on triangular mesh model [P], 2018.
[109] Y.S. Xu, T. Sebastian, L. Hoegner, et al., Voxel-based segmentation of 3D point clouds from construction sites using a probabilistic connectivity model, Pattern Recogn. Lett. 102 (2018) 67–74.
[110] D.J., Liu, Y. Yang, X.Y. Wang, & H.Z. Chen. Model voxelization efficiency optimization method and system based on CPU operation [P], 2020.
[111] G. Young, A. Krishnamurthy, GPU-accelerated generation and rendering of multi-level voxel representations of solid models. Comput. Graph-UK, 2018, 75(OCT.):11-24.
[112] J.P. Yuan, H. Li, B.H. Xu, G.X. Chen, Impact of Geometric Features on Color Similarity Perception of Displayed 3D Tablets, J. Imaging Sci. Technol. 64 (5) (2020) 1–12.
[113] P. Morovic, J. Morovic. Color Mapping in 3D Printing [P], 2019.
[114] M.K. Cho, H.K. Choh, S.E. Kim, Y.T. Kim, Y. Bang, Gamut mapping method for ICC saturated intent. In Color Imaging XII: Processing, Hardcopy, and Applications, International Society for Optics and Photonics. 6493 (2007) 64930K.
[115] J.P. Yuan, J.Y. Hardeberg, G.X Chen, Development and evaluation of a hybrid point-wise gamut mapping framework. In Proceedings of the Colour and Visual Computing Symposium, Gjovik, Norway, IEEE: Gjovik, Norway, 2015:1–4.
[116] L. Xu, B. Zhao, M.R. Luo, Colour gamut mapping between small and large colour gamuts: Part I. gamut compression, Opt. Express 26 (9) (2018) 11481–11495.
[117] M. Takeuchi, Y. Sakamoto, R. Yokoyama, S.U.N. Heming, Y. Matsuo, J. Katto, A Gamut-Extension Method Considering Color Information Restoration using Convolutional Neural Networks, in: In 2019 IEEE International Conference on Image Processing (ICIP) IEEE, 2019, pp. 774–778.
[118] D.L. Lau, G. Arce, Modern Digital Halftoning. (2001).
[119] X. Wang, M. Jiang, Z.W. Zhou, J.H. Gou, D. Hui, 3D printing of polymer matrix composites: A review and prospective, Compos. Part B-Eng 110 (2017) 442–458.
[120] J.P. Yuan, C. Chen, D.Y. Yao, G.X. Chen, 3D Printing of Oil Paintings Based on Material Jetting and Its Reduction of Staircase Effect, Polymers 12 (2020) 2536.
[121] J.P. Yuan, J.N. Tian, C. Chen, G.X. Chen, Experimental Investigation of Color Reproduction Quality of Color 3D Printing Based on Colored Layer Features, Molecules 25 (2020) 2909.
[122] J.N. Tian, J.P. Yuan, H. Li, D.Y. Yao, G.X. Chen, Advanced Surface Color Quality Assessment in Paper-based Full-color 3D printing, Materials 14 (4) (2021) 736.
[123] S. Gooran, F. Abedini, 3D Surface Structures and 3D Halftoning. Society for Imaging Science and Technology, 2020. Printing for Fabrication 2020, 2020. DOI: https://doi.org/10.2352/ISSN.2169-4451.2020.36.75.
[124] D. Defibaugh. 1997. The Collotype: History, process & photographic documentation. Rochester Institute of Technology (1997).
[125] F. Tang, W. Dong, Y. Meng, X. Mei, F. Huang, X. Zhang, O. Deussen, Animated Construction of Chinese Brush Paintings, IEEE T. Vis. Comput. Gr. 24 (12) (2018) 3019–3031.